SYNERGISTIC INDUCTION OF NRF-2 GENE BY CURCUMIN AND SULFORAPHANE AND PHARMACOKINETICS/METABOLISM OF I3C/DIM IN RATS BY UPLC/MS

by

Yury Y. Gomez

A Thesis submitted to the

Graduate School-New Brunswick

Rutgers, The State University of New Jersey

In partial fulfillment of the requirements

for the degree of

Master of Science

Graduate Program in Pharmaceutical Science

written under the direction of

Professor Ah-AN Kong, Ph.D

and approved by

_____

_____

_____

New Brunswick, New Jersey

January, 2011

ABSTRACT OF THE THESIS

PHARMACOKINETICS AND PHARMACODYNAMICS OF DIETARY CANCER CHEMOPREVENTIVE PHYTOCHEMICALS

By Yury Y. Gomez

Thesis Director: Ah-AN Kong

Curcumin (CUR) and Sulforaphane (SFN) have shown remarkable cancer chemopreventive effects in numerous studies and combinations of low doses of chemopreventive agents can reduce toxicity while augmenting efficacy. The first part of the thesis investigated the chemotherapeutic effects elicited by a combination of CUR and SFN on human hepatocarcinoma cells. The combination treatment- mediated effects on phase II/antioxidant enzymatic induction and antioxidant response element (ARE) was investigated. It was proposed that the combination of CUR and SFN could synergistically enhance the induction of ARE and the nuclear E2-factor related factor 2 (Nrf2)-mediated enzymes. Low doses of CUR and SFN significantly induced the expression of Nrf2-mediated enzymes, HO-1 and UGT1A1, promoted nuclear translocation of Nrf2– a key regulator of phase II detoxifying /antioxidant enzymes – and synergistically induced the ARE luciferase activity. Chemical inhibitors of mRNA and protein synthesis affected the combination therapy- mediated transcriptional regulation of both HO-1 and UGT1A1. Synergism of CUR and SFN was evident at low concentrations. Such synergism in ARE-luciferase activity may partly explain the significant induction in the expression of Nrf2- mediated expression of HO-1 and UGT1A1 and the nuclear translocation of Nrf2, suggesting that a combination of low doses may be a promising strategy for cancer chemoprevention. For the second part of this

thesis, a liquid chromatographic method was validated for the simultaneous analysis and pharmacokinetic evaluation of Indole-3-Carbinol (I3C), Diindolylmethane (DIM), and several I3C metabolites. I3C and DIM are naturally derived phytochemicals with promising *in-vitro* and *in-vivo* anticarcinogenic properties. Using reversed-phase ultra performance liquid chromatography (UPLC) coupled with mass spectrophotometry (MS), a rapid, specific, and high throughput method was developed and validated for the quantification and identification of I3C, DIM, and other I3C metabolites in plasma. Recovery, linearity, precision, accuracy, and stability analysis fulfilled the CDER guidelines criteria. The method was successfully applied to the determination of the pharmacokinetic parameters and elucidation of metabolites of I3C or DIM after oral, intravenous, or intraperitoneal administration to Sprague- Dawley rats.

ACKNOWLEDGEMENT

This work was partly supported by the National Institute of Health Grant RO1-CA073674.

I want to express my deepest gratitude to Dr. Ah-Ng Tony Kong for his continuous advice and support during my time at his lab. I would like to especially thank Avantika Barve for her great support, advice and patience particularly during the first part of my thesis. I wish to thank all who aided in one way or another in the review of this thesis, especially members of Dr. Kong's lab for their time, input, and advice. I am also very grateful to McNeil Consumer Healthcare (PA) for their permission to use the UPLC/MS spectrophotometers as well as for providing me access to the WinNonlin modeling software, and to the members of the analytical R & D group, for their helpful insight into UPLC technology. I owe my deepest gratitude to my family who offered me their unconditional support throughout all this time. I also wish to show my immense gratitude to my friends and colleagues for their continuous moral support and encouragement.

DEDICATION

I wish to dedicate this thesis to my husband, my sons, my siblings, and my friends. Their love, support, and guidance have continuously motivated me and inspired me to be the person I am today. This work is especially dedicated to the memory of my mother (1952-1992), who lost the battle against Amyotrophic Lateral Sclerosis leaving nine children behind. Very especially, I wish to dedicate this work to all kinds of minority students who come from underrepresented countries and who day after day struggle hard to persevere with their goals sacrificing their personal time, life, and family. May this work also serve as an inspiration to parentless students who must succeed on their own and seek their own support. Lastly, I dedicate this work to all patients affected by cancer that are faithfully awaiting a cure for their desperate disease. May this piece of work, hopefully, contribute a little seed into a better understanding of cancer and lead scientists someday to gloriously say there is a cure.

TABLE OF CONTENTS

CHAPTER 3

Development and Validation of a Rapid UPLC/MS Method for the Simultaneous Determination of I3C, DIM, and Related Metabolites and its Application to Pharmacokinetics in Rats

LIST OF TABLES

LIST OF FIGURES

CHAPTER 1

Introduction

1.1 Carcinogenesis Background

Cancer development and progression involves several complex mechanisms including initiation, stepwise progression, and metastasis. The latter three critical steps can ultimately lead to the rapid proliferation and uncontrolled growth of cancerous cells that can affect other parts of the body [1]. Significant efforts have been made over the last decades to reduce cancer mortality, yet promising therapies against this deadly disease are still poor [2] and a better approach seems to be early diagnosis of malignant tumors as well as cancer prevention. Prior to becoming malignant, tumors go through long-lasting pathological molecular changes including pre-neoplastic and premalignant stages [3]. For this reason, a better strategy for tumor prevention, delay, or arrest prior to progression into more advanced stages includes changes in lifestyle (i.e. diet) and treatment with cancer chemopreventive drugs [4].

1.2 Stages of Carcinogenesis

It is well known that carcinogenesis is a very complex process by which normal cells become malignant (Fig 1.1). Such process is often characterized by alterations in structure and function of the genetic code (DNA) through mis-regulation of multiple cell signaling pathways [5]. Cancer onset is normally accompanied by cell transformation, gene mutation, carcinogen metabolism, and aberrant DNA repair. Normally, this initiation stage is induced by environmental carcinogens such as tobacco, pollution, or certain dietary agents that result in simple genetic mutations, transitions, or deletions, which in turn are responsible for the regulation of carcinogenic processes. Important mechanistic pathways for cancer initiation

involve enzymatic biotransformation (i.e. cytochrome P450 system) of pro-carcinogens into active carcinogens as well as the oxidative metabolism of xenobiotic compounds into reactive oxygen species (ROS) that can bind DNA. Fortunately, pivotal systems exists that aid in the detoxification of activated carcinogens (i.e. Phase II systems such as glucoronidases, sulfotransferases) or in DNA repair mechanisms to overcome DNA damage as a result of carcinogen-DNA adduct formation or mistranslation of the genetic material [5]. Bioactive compounds such as indoles, resveratrol, genistein, and compounds from cruciferous vegetables have shown remarkable anti-initiation properties [6]. Promotion occurs when there is a dysfunction of signaling pathways responsible to control cell proliferation and apoptosis. Normally, human cancers have mutations in the genes that regulate cell cycle. For instance, in pancreatic tumors, p27 mutations are normally encountered, whereas in colon cancers, p53 mutations often prevail. Such genetic mutations generally lead to an eminent dysfunctional cell death system marked by continued proliferation of the mutated cells to a point where cancerous cells outnumber normal cells. Contrary to initiation, cancer promotion is a reversible stage and hence great interest exists in finding agents that can arrest or reverse this stage. Some of the target molecular pathways involved in promotion include hormone receptors, cell cycle check point markers, transcription factors, mitogen-activated protein kinases (MAPK), cell junctions, tumor suppressor genes among others [5]. Further genetic alterations can ultimately lead to tumor progression often characterized by accumulation of mutated genes and chromosomal abnormalities. Cancer progression is therefore a stage marked by invasion, angiogenesis, and metastatic growth. Some compounds with known biological activity and inhibition potential against angiogenesis include polyunsaturated fatty acids, EGCG, resveratrol, curcumin, and genistein [5].

1.3 Cancer Current Statistics and Epidemiology

Cancers of the lung and bronchus, prostate, and colorectum, and breast are the most common fatal types of cancers among men and women. According to the National Institute of Health report for 2010, the projected number of cancer-related deaths for 2010 for American men and women is estimated to be approximately 569,490 which correspond to 1 in 4 deaths [7]. However, over the last three decades, cancer survivor patients in the United States have escalated from 3 million to 9.8 million, which is equivalent to about 3.5% of the population. Such increase in survival rate has been possible thanks to the great strides in early diagnosis, more effective treatment, disease prevention, and decrease in mortality from other reasons. Clear evidence of such progress was seen by a 64% increase in survival rate of cancer-diagnosed adult patients for a 5-year anticipated survival period in 1995-2000 [8].

1.4 Cancer Risk Factors

Literature indicates that environmental pollution including water and air pollution is associated with great cancer mortality rates [9]. Others studies have pointed at an increased risk to develop lung cancer for those individuals with genetic polymorphisms [10] and for tobacco smokers [11]. Additional factors involved in cancer etiology include environmental exposures, diet, alcohol, physical inactivity, stress, environmental carcinogens, and infectious agents [12].

1.5 Cancer Chemoprevention

The term ‘chemoprevention’ was coined in the late 1970s and has since been used to refer to the use of naturally derived phytochemicals for the prevention of cancer [13]. Great scientific interest has been placed in the molecular targeting of such chemopreventive agents to elucidate potential mechanistic modes of action toward the prevention of cancer [5]. Natural chemopreventive phytochemicals are commonly found in food [14]. Numerous studies have

pointed out at the great benefits and potential of a diet rich in vegetables and fruits in reducing the incidence of various cancer types [15-18]. Vegetable and fruit-derived vitamins and micronutrients as well as other chemicals derived from natural plants can aid in the prevention of cancer initiation by offsetting the detrimental effects of mutagens, carcinogens, and tumor promoters. Chemoprevention by these natural cancer inhibitors is preferred over the use of synthetic compounds due to the apparent reduced toxicity of natural agents. Additionally, in spite of the general knowledge on the effects of natural products on the reduction of carcinogenesis incidence and the significant progress into the comprehension of its multistage nature, there is still a marked gap in the understanding of the most effective diet constituents as well as in the elucidation of the molecular mechanisms involved [19]. Dietary compounds such as carotenoids (i.e. β-carotene, lycopenes), flavonoids (i.e. quarcetin, kaempferol, green tea catechins (-) epigallocatechin-3-gallate (EGCG)), genistein, turmeric spice (i.e. curcumin), gingerols, resveratrol and isocyanates such as sulforaphane (SFN), phenylethyl isocyanate (PEITC), are the major dietary types of anticancer chemopreventive agents. Dietary sources for all these compounds include grapes, wine, tomatoes, soy products, garlic, cabbage, broccoli, onions, peppers, rice, wheat, carrots, celery, and turmeric spice among others [1]. All these compounds elicit their chemopreventive actions by activating cellular defense systems with detoxifying and antioxidant potential, inhibiting anti-inflammatory pathways, and inducing cellular apoptosis or cell cycle arrest [1]. Studies have linked the reduced risk in cancer occurrence to the consumption of green tea. *In vitro*, EGCG arrested cancer growth and promoted apoptosis in various human cancer cell lines of melanoma, breast, leukemia, lung, and colon as reviewed by Pan et al [1]. Tumor incidence was also reduced in Apc (Min/+) mice fed with PEITC. The mechanistic inhibition was shown to be related to induction of apoptosis via up-regulation of

cleaved caspases and PARP and cell cycle arrest via down-regulation of several types of cyclins biomarkers or activation of p21 [20]. Thus far, the mouse skin model has provided great understanding of multistage carcinogenesis and has allowed differentiation of the three stages: initiation, promotion, and progression [21, 22].

Cancer chemopreventive compounds that interfere with carcinogens and thus prevent them from reaching critical targets are called blocking agents, whereas chemopreventive agents that can halt the evolution of cancer cells into more advanced neoplastic stages are known as suppressing agents [23]. Cancer chemoprevention by blocking agents has been linked to an increase in the mechanistic activity for detoxification of carcinogenic xenobiotics, tumor promoters, and tumor progressors. Two important pathways accountable for such detoxifying mechanisms include phase I and phase II enzymatic systems. By means of the oxidative, reductive, and hydrolytic properties induced by phase I reactions or through conjugation reactions caused by phase II reactions, such systems can modify the polarity or hydrophilicity of carcinogenic substances, thus improving their excretion capability. Some important phase II detoxifying systems include glutathione-S-transferases (GST) and UDP-glucoronosyltransferases (UGT), which can form conjugates with reactive endogeneous and exogeneous electrophilic/nucleophilic metabolites resulting upon activation of invading carcinogens such as polycyclic aromatic hydrocarbons, nitrosamines, aromatic amines, fungal toxins, steroid hormones, etc. UGTs are commonly found in the endoplasmic reticulum and nuclear membranes in close proximity to the genetic material, suggesting its important protective role in the deactivation of mutagenic and carcinogenic endogeneous and exogeneous compounds [19]. Furthermore, there is evidence supporting the relationship of oxidative stress arising from reactive oxygen species (ROS), inflammation, and apoptotic cell cycle deregulation with all stages of carcinogenesis [1]. ROS species such as

hydroxyl, peroxy, and superoxide anion radicals as well as singlet oxygen cause damage to DNA (i.e. base alterations, strand breakage, mutations, etc), proteins, and lipids. These processes occur naturally as result of environmental exposures such as sun ionizing radiation or pollutants or lifestyle, or biological processes (i.e. mitochondrial electron transport). Cellular attack by ROS can influence cellular signaling cascades and elicit changes in the activation or expression of transcription factors and upstream kinases [1]. It becomes clear, then, that key mechanisms for anti-tumor prevention or inhibition need to be targeted against: inhibition of inflammation, inhibition of cell proliferation, modulation of cell differentiation and cell death, scavenging of ROS, and boosting of antioxidant defense systems as well as detoxification pathways [19] (Table 1.1).

1.5.1 Curcumin- Chemical properties and molecular chemopreventive pathways

Curcumin (CUR) is derived from the dietary spice turmeric (*Curcuma Longa*). Abundant literature has pointed at its beneficial roles in anti-inflammation, anti-oxidation, chemoprevention, and chemotherapeutic activity as demonstrated not only in cultured cell experiments but also in animal models [24]. CUR extracts are typically a mixture of at least three related structures including CUR, demethoxy curcumin, and bismethoxy curcumin. There is still high uncertainty as to which component is the most potent as an antioxidant and antitumor agent. CUR is poorly soluble in water, slightly soluble in methanol, and highly soluble in DMSO and chloroform. Such poor polar solubility has been attributed to its low *in vivo* bioavailability in clinical trials. Furthermore, since CUR exists as a mixture and exhibits different potencies, the amount of CUR in experimental studies is often not accurately determined. CUR has high lipophilicity which is a favorable feature for rapid cell permeation. Furthermore, CUR is a free

radical scavenger, a reducing agent, and DNA-disrupting agent in the presence of Cu and Fe ions. Such features contribute to its pro- and anti-oxidant biological activity [24].

According to a recent review by Hatcher et al. (2008), CUR was capable of suppressing acute and chronic inflammation in vitro where it blocked lipo-oxygenase and cyclo-oxygenase-inflammatory activities induced by Phorbol 12-mystistate 1-acetate (PMA) in mouse fibroblast cells, nitric oxide production in RAW 264.7 murine macrophages, and reactive oxygen species (ROS) generation in activated rat peritoneal macrophages. Generation of pro-inflammatory cytokines such as interleukin-8 (IL-8), monocyte inflammatory protein-1 (MIP-1), monocyte chemotactic protein-1 (MCP-1), interleukin-1β (IL-1β), and tumor necrosis factor-α (TNF-α) was also inhibited by CUR. The chemopreventive ability of CUR in arresting cancer development and progression is related to its ability to both inhibit cancer initiation, by preventing carcinogen activation, and suppress malignant cell proliferation during promotion and progression stages. Dose-dependent chemotherapeutic effects elicited by CUR have been established in various animal studies of colon, duodenal, stomach, esophageal, and oral tumorigenesis. Very interestingly, CUR also functions as a chemosensitizer agent and therefore can augment the activity of other anti-neoplastic compounds through inactivation of pathways that contribute to therapy resistance. Of equal importance is the dual ability of this compound to exert both radioprotective effects in normal cells and radiosensitizing effects in cancerous cells. It has been hypothesized that its radioprotection ability may be linked to its potential for reducing oxidative cellular stress as well as for its ability to block gene transcription, otherwise needed for oxidative stress and inflammatory response, and that its radiosensitizing effect is rather due to gene induction involved in apoptosis. Some of the target-signaling pathways of CUR include key survival pathways controlled by NFκB and Akt as well as Nrf2-mediated

cytoprotective pathways. Akt is a protein kinase that enhances cell survival by blocking cell death via activation of phosphorylation mechanisms. Inflammation-causing gene products generated by the NFκB-regulated pathway include cyclo-oxygenase-2 (COX-2), cyclin-D1, adhesion molecules, MMPs, inducible nitric oxide synthase, Bcl-2, Bcl-$_{xL}$ and TNF-α. Under normal conditions, NFκB proteins are sequestered in the cytoplasm in an inactive state, but upon inflammatory activation are translocated to the nucleus via activation of various kinases and through phosphorylation and degradation of IκB (the NFκB cytoplasmic inhibitor). CUR exerts its pleitropic effects by inhibition of the NFκB pathway and downstream signal transduction proteins (i.e. COX-2, Cyclin D1, etc), which in turn play critical roles in tumor promotion, cell cycle proliferation, as well as gene amplification or translocation. Additional chemoprotective effects by CUR include induction of phase II enzymes such as NAD(P)H:quinone reductase, heme oxygenase (HO), and Glutathione (GSH), which are in turn responsible to prevent or reduce carcinogen-induced cellular stress [24].

1.5.2 Sulforaphane - Chemical Properties and Molecular Chemopreventive Pathways

Sulforaphane (SFN) is a type of isothiocyanate (ITC) which can particularly be obtained from broccoli consumption [25]. ITCs are generated by hydrolytic reactions of glucosinolates, metabolites of SFN, by means of intestinal microflora [26]. SFN has been implicated in protective anti-tumorigenic effects in rodents. The incidence, multiplicity, and rate of formation of mammary tumors induced by dimethylbenz(*a*)anthracene (DMBA) in rats was greatly minimized after a diet of broccoli sprouts [27]. Furthermore, SFN inhibited multiplicity of carcinogen-induced hyperplasias in pancreatic ducts [28]. It also suppressed the expansion of malignant crypt foci in colon carcinomas [29] and delayed the proliferation of PC-3 human

prostate cancer xenografts in nude mice [30]. Therefore, SFN is a versatile naturally occurring agent with exceptional ability to prevent or arrest cancer at various post-initiation stages [25]. The paramount SFN-mediated chemopreventive foundations embrace multiple cross-interacting mechanisms that can overcome the risk of tumorigenesis. Such mechanisms entail inhibition of phase I and phase II metabolizing enzymes, antioxidant regulatory functions, induction of apoptosis and cell cycle arrest, inflammation-controlling properties, and hindrance of angiogenesis [25]. Carcinogen metabolism by phase I reactions, through hydrolysis and reduction, generate more hydrophilic species that are readily metabolized by cytochrome (CYP) P450 enzymes. Phase I metabolism renders the pro-carcinogen species into very highly reactive species that can easily bind DNA, RNA, and protein. Phase I metabolism is a mechanism involving ligand-receptor interactions. For example, ligands (i.e. procarcinogens) can bind the Aryl hydrocarbon (Ah) receptor forming a complex that can subsequently be transported to the nucleus and bind to the xenobiotic responsive element (XRE), in turn responsible for expression of CYP P450 enzymes. Numerous studies in rodents have revealed the efficacy of SFN at halting DNA-adduct formation by modulating the levels of CYP P450 isoforms via a competitive-based inhibition mechanisms or direct covalent modification [31, 32]. SFN also showed potent enzyme inhibition, namely CYP2E1, in liver microsomes against genotoxic effects of N-nitrosodimethylamine (NDMA) [33]. Another crucial mechanism for the chemopreventive effects of SFN is related to its ability to induce phase II enzymes, which can inactivate carcinogens and make them readily available for excretion. SFN-mediated cytoprotection through phase II machinery can enhance conjugation reactions of endogenous ligands, including GSH and glucoronic acid, to endo and xenobiotic carcinogens, thus conferring cytoprotection against ROS [25]. In vitro studies using human HepG2 liver cells have demonstrated the

efficacy of SFN to induce several phase II genes such as NAD[P]H: quinone oxydoreductase (NQO1), GST, and UGT ,which ultimately can lead to the expression of important gene products such as UGT1A1 or heme oxygenase-1 (HO-1) [25, 34]. Modulated expression of phase II enzymes is transcriptionally controlled by the antioxidant response element (ARE), which is found in the promoter regions of these genes [35]. An essential component for the ARE- binding transcriptional machinery is the NF-E2-related factor (Nrf2), which belongs to the cap'n'collar family of basic leucine zipper (bZIP). Experiments conducted in Nrf2 deficient mice showed a dramatic downregulation in antioxidant/detoxifying enzyme expression, while experiments using Nrf2 knockout mice showed a higher susceptibility for promotion of carcinogenesis. The latter studies, thus, added proof to the crucial role of Nrf2 in such inhibitory process [36-38] and Nrf2 is currently considered a novel molecular target for cancer chemoprevention [39]. All the above provides evidence of the potential of SFN to regulate xenobiotic-metabolizing enzyme systems via up-regulation of carcinogen-detoxifying machineries. Figure 1.2 provides a scheme of the molecular signaling cascades involved in carcinogen metabolism and the modulatory influence of dietary agents in the pathway.

1.5.3 Indole-3-Carbinol and Diindolylmethane - Chemical Properties and Molecular Chemopreventive Pathways

Indole-3-Carbinol (I3C) is a phytochemical normally found in cruciferous vegetables and has been shown to exhibit anticarcinogenic properties in several animal models and in various cell lines [40-42]. I3C is found in the form of glucosinolates naturally derived from vegetables of the family cruciferae and brassica. Vegetables of this type include all kinds of cabbage, broccoli, cauliflower, and brussel sprouts. By means of hydrolysis, glucosinolates form unstable isocyanates which result in the production of I3C [43]. Additionally, I3C has great biological

activity and under acidic conditions is readily converted into 3,3-diindolylmethane (DIM), which is also biologically active [44]. I3C and DIM are capable of up-regulating expression of phase I and phase II enzymatic systems responsible for the detoxification and inhibition of carcinogens. In prostate and breast cancer cells, I3C has shown inductive effects of G1 cell cycle arrest and apoptosis and microarray gene expression profiling has shown evidence of the important effects of I3C and DIM in the regulation of genes that control cell cycle, cell proliferation, signal transduction, and other cellular processes [45, 46]. Some of the molecular mechanisms by which I3C exerts its effects are related to inhibition of Akt and nuclear factor NFκB, which are essential components for cell survival and are thus potential targets in cancer therapy [45]. As reviewed by Sarkar et al. [45], NFκB exerts control on the expression of genes that regulate cell proliferation, differentiation, apoptosis, inflammation, stress response, angiogenesis, tumor progression, and metastatic invasion. Since NFκB is believed to play a critical role in tumor development, inhibition of this factor is considered crucial for blocking tumorigenesis. Induction of apoptosis by these I3C and DIM was found to be linked to a reduction in Bcl-2 and Bcl-xL expression and to up-regulation of Bax [45]. Bax is believed to be responsible for apoptotic cell death, while Bcl-2 and Bcl-xL is believed to block cells from apoptosis [47]. Inactivation of these two latter factors with chemopreventive agents I3C and DIM have resulted in sensitization of otherwise resistant cancer cells, and therefore provide a novel breakthrough into the potential to develop novel cancer therapies [45]. To date, only few studies have evaluated the pharmacokinetics and disposition of I3C or DIM in rodents and humans [48-51], but have done so only following oral administration. Also, even though several metabolites of I3C have been identified, none of those studies provide detailed information on the pharmacokinetics of those metabolites nor do they show the pharmacokinetic metabolic profiles.

1.6 Combination Therapy as a More Effective Chemopreventive Approach

Recently, great interest has been placed in the study of the effects of multiple drugs as chemopreventive treatments. It is believed that by concomitantly directing therapies at multiple cellular targets, multiple subpopulations, or multiple diseases, several mechanisms or modes of action can be activated which can either separately provide the pharmacological effects to each single target or disease or simultaneously act to enhance the effectiveness of such effects to treat a target or disease. The latter option offers significant benefits in disease intervention such as improved efficacy of the therapeutic effect, a possibility to decrease the dosage while maintaining or increasing the efficacy and therefore reduced toxicity, diminished drug resistance, and potential selective synergism against the target [52]. Several studies using chemopreventive compounds against cancer have demonstrated synergism and enhanced effectiveness when combining several agents. A combination study of SFN and EGCG in HT-29 cells showed synergism [53]. Also when combined, SFN and dibenzoylmethane (DBM) resulted in a synergestic effect *in vivo* [54] and CUR and SFN synergistically up-regulated the expression of HO-1 and improved the antioxidant properties by reduction of inflammatory molecules [55].

1.7 Approaches for Metabolic Profiling

High throughput screening approaches are recently being used by many pharmaceutical companies to accelerate the drug discovery process of new chemical leads. The increasing need for selection of robust drug candidates that possess acceptable balance between potency, safety, efficacy and pharmacokinetics has prompted investigators to focus on drug metabolism and pharmacokinetic (DMPK) studies in the early discovery process as it became clear that success strictly relies upon selection of suitable DMPK drug behavior. Typically, several hundred million dollars are invested in drug discovery and development and hence identification and selection of

processes that aid in robust candidate selection are badly needed. It is estimated that about 46 % of drug leads were dropped from clinical development phase due to unacceptable efficacy and about 40% did not meet safety requirements. It becomes then evident that understanding human pharmacokinetics such as oral bioavailability, half life, drug plasma-protein binding, etc. at the early drug discovery phase provides great value in reducing such preclinical and clinical failures [56].

Some of the *in vitro* screening methodologies to study DMPK characteristics include absorption models (i.e. Caco-2 human intestinal cell line, which has shown great usefulness in the prediction of *in vivo* human intestinal absorption), transporter models (i.e. P-gp, L-MDR1, which can provide important information of the potential contribution of transporters to the disposition of drugs), *in-silico* models (capable of predicting absorption based on the drug's physicochemical data such as log P, pKa, and solubility), metabolic stability models (i.e. cytochrome P450 reactions, which can determine the presence or absence of first pass intestinal or liver metabolism and hence the oral bioavailability) [56].

Many of the *in vivo*, *in vitro*, and *in silico* screening assays would not be possible without the integration of technological advances in computing, automation, sample preparation, as well as sensitive and selective detection systems. One of the most striking advances has been the invention of LC/MS/MS technology which offers excellent capability for high throughput analysis and elucidation of metabolites [56, 57]. While high throughput analysis is often hindered by the need to develop analytical assays for each single drug, careful selection of the analytical methodologies can have a significant impact on the throughput of DMPK screening [56]. Reverse phase liquid chromatography (RP-LC) typically uses narrow bore columns with particle sizes ranging between 3-5 μm. Nonetheless, conventional RP-LC separation is

frequently unsuitable and insufficient for the separation of complex biological matrixes, causing inadequate metabolite resolution. A recent innovative approach is the use of ultra performance liquid chromatography (UPLC) which provides greater chromatographic resolution and peak capacity as a result of small column particle size (i.e. 1.7 μm). The use of sub-2μm particles results in narrow chromatographic peaks providing enhanced resolution and improved detection limits [58].

1.8 Summary

The process of carcinogenesis is very complex and includes several stages of development: initiation, promotion, and progression. However, studies carried *in vitro* as well as *in vivo* have indicated that tumorigenesis can be intervened by treatment with dietary phytochemicals. Natural agents can prevent cancer by acting as blocking agents of the initiation stage. Phytochemicals have the potential to inhibit carcinogen-induced cellular damage, counteract ROS generation, or inhibit radiation-induced DNA mutagenesis. Furthermore, chemopreventive compounds have been shown to be excellent inhibitors of procarcinogens by blocking their activation via down-regulation of CYP 450 enzymes involved in the activation process. They can also turn on mechanisms of procarcinogen antioxidation or detoxification by inducing the expression of Phase II enzymes via the Nrf2/ARE signaling pathway. Cancer intervention after the post-initiation stage is more complex and not fully understood owing to the multiple cellular signaling pathways involved as well as to the unique interactions and effect relationship between molecular receptors and each chemopreventive agent.

Abbreviations: DIMO, di-1 H-indol-3-ylmethanone; DIMOH, di-1H-indol-3-ylmethanol; ICZO**,** indole-[3,2*b*]-carbazole-6,12-(5*H*,11*H*)-dione.

Additionally, recent studies have shown increased chemopreventive efficacy when combining several chemopreventive agents. Such an approach allows the use of smaller doses and can diminish the toxic effects of high dosing regimens. When evidence resulting from both in vitro and in vivo studies indicates good potential and efficacy of chemopreventive agents for treating any cancer, interests may arise to move from preclinical to clinical investigations. Clinical investigations, however, involve human subjects and therefore clear evidence of the compound's safety is necessary prior to entering that phase. DMPK studies are therefore necessary to evaluate the efficacy and safety of any drug prior to moving into the clinical phase. DMPK provides a venue into the understanding of the behavior of the parent drug *in vivo* and its results can be used to extrapolate or predict the drug's efficacy and safety in humans.

Due to the increasing evidence on the anti-tumorigenic effects of CUR and SFN, and also owing to the recent interest in studying the combinatorial effects of therapies that use two or more chemopreventive agents to improve treatment efficacy, the second chapter of this thesis was aimed at investigating the combinatorial effects of CUR and SFN as chemopreventive agents. Furthermore, since one successful strategy for cancer intervention is the modulation of drug metabolizing enzymes which can facilitate the elimination of endogenous and xenobiotic carcinogenic species using natural chemopreventive agents, the second chapter investigated the enzymatic induction of important phase II antioxidant/detoxifying systems including UGT and HO enzymes. Also, since multiple studies have shown that induction of phase II systems is regulated by the Nrf2/ARE-mediated gene transcription, the implication of such molecular targets in the chemopreventive treatment with the combination agents was studied. The results, after western blotting or mRNA analysis, indicated that by combining low doses of CUR and SFN, there was a significant induced expression of Nrf2-mediated enzymes including HO-1 and

UGT1A1 compared to treatments that used each chemopreventive agent alone. Using chemical inhibitors of mRNA and protein synthesis, it was observed that a combination of CUR and SFN affected the transcriptional regulation of both HO-1 and UGT1A1. Additionally, the combination of CUR and SFN resulted in the nuclear translocation of the Nrf2 and synergistically induced the ARE luciferase activity. All these results indicated that synergism arising from combining CUR and SFN exists at low concentrations suggesting that a combination of low doses may be a promising strategy for cancer chemoprevention.

I3C and DIM have shown remarkable chemopreventive effects both *in vitro* and *in vivo* and several clinical studies have evaluated the pharmacokinetic disposition of such agents after oral administration. However, the bioavailability of I3C is very low due to the high extent of first pass metabolism as a result of the acidic environment in the stomach. The latter observation makes evaluation of alternate administration routes imminent. Also, one of the major metabolites of I3C is its dimerization product DIM, yet there is limited pharmacokinetic data for such compound. The third chapter of this thesis describes the development and validation of a rapid UPLC/MS chromatographic method for the sensitive determination of I3C or DIM in rat plasma after administering these drugs, via several parenteral administration routes including intravenous (i.v.), intraperitioneal (i.p.) or oral (p.o), to Sprague Dawley rats. The method was applied to the evaluation of the pharmacokinetic parameters of the parent drugs (I3C or DIM) as well as to the evaluation of the major metabolites of I3C observed in various administration routes. The mean recovery was 96.21 % for I3C and 108.5% for DIM. The run time was 9 minutes in contrast to a 60 minute run time for an existing HPLC method. The limits of detection and quantification for both I3C and DIM were 10 ng/mL and 25 ng/mL respectively. The method showed excellent linearity ($r > 0.99$), precision, accuracy, and stability in plasma. At least three

metabolites not previously reported (DIMO, DIMOH, and ICZO) before were proposed in the current studies. Evidently, metabolic bio-transformation of I3C was very rapid and the concentration of most metabolites was clearly higher than that of I3C at all time points including initial timepoints.

The concentration-time profiles after i.v. or i.p. administration of I3C as well as after i.v. administration of DIM clearly exhibited multi-exponential concentration decline with rapid distribution and absorption phases and slow first order elimination. On the other hand, the oral PK profile of DIM exhibited slow absorption phase and slow mono-exponential first order decay. Two-compartment pharmacokinetic models fitted the plasma concentration -time profiles of DIM or I3C after i.v. and i.p. administration very well and one compartment model described the pharmacokinetic data of DIM following oral administration. Pharmacokinetic parameters and profiles are presented for both parent drugs and metabolites. DIM was poorly bioavailable after oral administration given as a polymer suspension, yet no DIM metabolites were encountered upon analysis. These are the first studies to show absolute bioavailability of DIM in rats based on i.v. and p.o. dosing regimens. Also, the apparent terminal half life after oral administration of DIM was significantly longer than reported in literature for absorption enhanced DIM formulation and resembled a slow-release PK profile. Administration of 50 mg/kg of I3C (i.p) in a DMSO/oil formulation showed striking increased systemic exposure compared to the administration of 100 mg/kg of I3C (i.p) in a polymer formulation, and also resulted in less metabolites than when administered by an i.v. route. Such observations pointed out at a marked advantage for regional i.p. delivery of I3C using such drug delivery vehicle.

Due to the relatively short run time, the method will allow high throughput analysis of pharmacokinetic samples and will ease development and validation of other UPLC methods for

analysis of I3C and related compounds in other biological matrixes. Also this study makes clear that UPLC/MS provides an excellent opportunity for the elucidation of new metabolites unable to be resolved by conventional HPLC. This benefit, in turn, will generate new inroads into the understanding of the true metabolic fate of compounds.

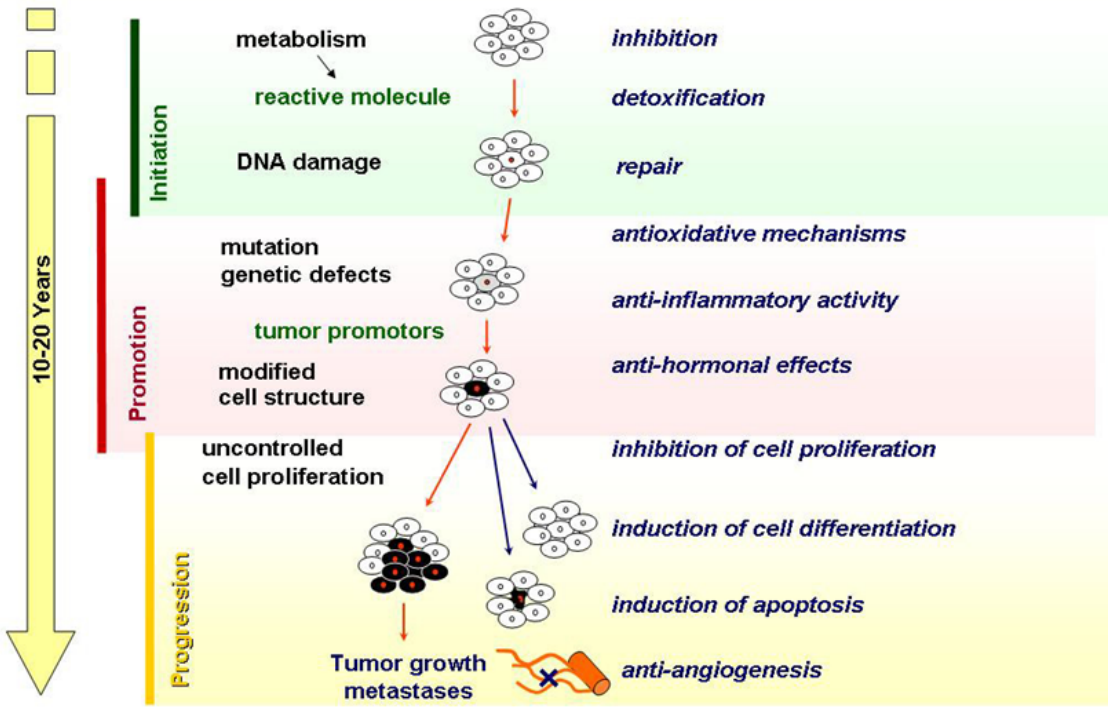

Figure 1.1. Carcinogenesis from Initiation to Metastasis[1]**.** Tumor formation results from an accumulation of genetic and biochemical cell damage, which renders the need to discover chemopreventive agents that can target carcinogenesis at various stages, thus offering the potential for prevention, inhibition, or slow promotion from early genetic lesions to late stage tumor growth. Target molecular mechanism include modulation of carcinogen metabolism by means of antioxidant, radical scavenging, anti-inflammatory, cell cycle arrest, anti-proliferative systems, and induction of cell death. Understanding of the molecular mechanisms provides the grounds for safe application of existing chemopreventive agents as well as for development of future anti-cancer agents.

[1]http://www.dkfz.de/en/tox/c010-2_projects/list_assays.html [59]

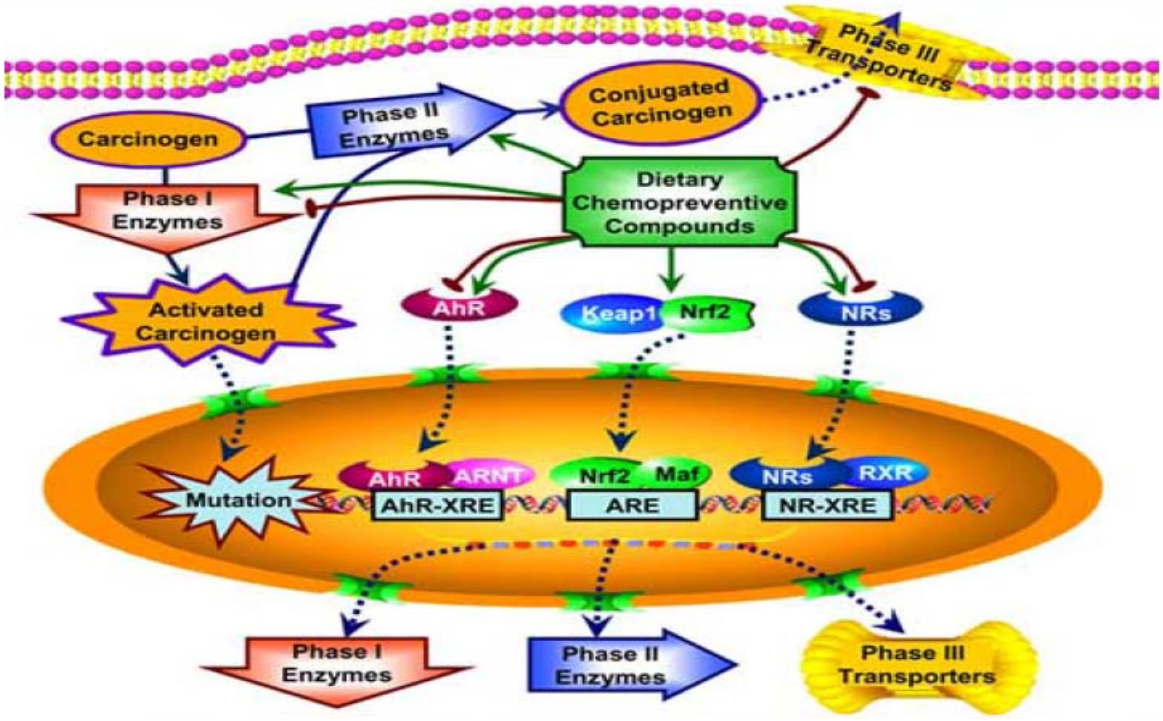

Figure 1.2 Molecular Targets for carcinogen-induced metabolism and mechanistic modulation by chemopreventive agents[2]**.** Naturally occurring phytochemicals can influence cancer development by either mechanistically promoting or blocking the expression of metabolizing enzymes and cellular transporters via important nuclear receptors and Nrf2 mediated signaling cascades or by targeted activation and abrogation of enzymes and transporters involved in carcinogen metabolism.

[2]Yu, S. & Kong, A-N. (2007). Current Cancer Targets 7, 416-424.

Table 1.1 Stage-Specific Carcinogenesis Targeting by Chemopreventive Compounds[3]

Mechanisms of Prevention	*Examples of Preventive Agents/Factors*
Tumor Initiation	
a. Inhibition of phase I enzymes to prevent the formation of reactive carcinogenic metabolites	a. Epigallocatechin gallate (EGCG), selenium, phenylisothiocyanate (PEITC), indol-3-carbinol, coumarins, ellagic acid, resveratrol, genistein, 1-ethynylpyrene
b. Inhibition or induction of oxidative enzyme pathways to produce less carcinogenic metabolites	b. Butylated hydroanisole (BHA), butylated hydroxytoluene (BHT), ethoxyquin, 7,8-benzoflavone, quercetin
c. Enhancement or induction of detoxification enzymes (phase II enzymes) and pathways	c. Oltipraz, EGCG, PEITC, diallyl sulfide, resveratrol, *N*-acetylcysteine, D-glucarate
d. Direct chemical scavenging of carcinogenic intermediates	d. Ellagic acid
e. Inhibition or enhancement of DNA repair	e. Calorie restriction, EGCG, selenium
f. Inhibition of cell proliferation and DNA synthesis	f. Calorie restriction, difluoromethylornithine, selenium, antiestrogens, dehydroepiandrosterone (DHEA), fluasterone, retinoids, D-glucarate
Tumor promotion/progression	
a. Inhibition of inflammation	a. Nonsteroidal anti-inflammatory drugs, calorie restriction, DHEA, fluasterone, antihistamines, resveratrol, ursolic acid, avicins
b. Inhibition of cell proliferation and hyperplasia	b. Calorie restriction, difluoromethylornithine, selenium, antiestrogens, DHEA, fluasterone, retinoids, D-glucarate
c. Modulation of cell differentiation and apoptosis	c. Retinoids (*all-trans* retinoic acid, fenretinide), calorie restriction, monoterpenes (that is, D-limonene), fluasterone, genistein, calcium
d. Scavenging of reactive oxygen species and preventing depletion of antioxidant defense systems	d. Antioxidants (carotenoids, α-tocopherol, ascorbic acid, proanthocyanidins, EGCG, avicins), selenium, calorie restriction
e. Detoxification of tumor promoters, especially steroid hormones	e. D-Glucarate, aromatase inhibitors, antiestrogens

[3]Hanausek, M., Walaszek, Z. & Slaga, T. (2003). *Integrative Cancer Therapies* **2**, 139-144.

CHAPTER 2

Nfr2-mediated Antioxidant and Detoxifying Enzyme Induction by a Combination of Curcumin and Sulforaphane[1,2]

2.1 Abstract

Background Curcumin (CUR) and sulforaphane (SFN) have shown remarkable cancer chemopreventive effects in numerous studies. There is also an increasing interest in the use of combinations of low doses of chemopreventive agents that exhibit distinct modes of action as opposed to administering high doses of a single agent as this conceptualization can reduce toxicity while augmenting efficacy.

Purpose This study was aimed at investigating both the phase II/antioxidant enzymatic induction ability of combined low doses of CUR and SFN and the effect of the combination treatment on the antioxidant response element (ARE) in HepG2-C8 cells. It was proposed that combination of polyphenol CUR and isothiocyanate SFN could synergistically enhance the induction of ARE and the nuclear factor (erythroid-derived 2)-like 2 (NFE2L2 or Nrf2)-mediated enzymes.

Methods HepG2-C8 cells were treated with a combination of low doses of SFN and CUR or each drug alone. The induction of the Nrf2-mediated antioxidant and phase II detoxifying enzymes – heme oxygenase-1 (HO-1) and UDP-glucoronosyl transferase-1A (UGT1A) – was measured by Western blotting and reverse transcription- polymerase chain reaction (RT-PCR). The ARE luciferase activity was also measured.

Results Low doses of CUR (10μM) and SFN (12.5 μM) significantly induced the expression of Nrf2-mediated enzymes HO-1 and UGT1A1. Using chemical inhibitors of mRNA and protein synthesis, we observed that a combination of CUR and SFN affected the transcriptional

regulation of both HO-1 and UGT1A1. Additionally, a combination of CUR and SFN resulted in the nuclear translocation of the Nrf2– a key regulator of phase II detoxifying /antioxidant enzymes. Lastly, the combination of CUR and SFN synergistically induced ARE luciferase activity.

Conclusions Synergism of CUR and SFN exists at low concentrations. The synergism in ARE-luciferase activity may partly explain the significant induction in the expression of Nrf2-mediated expression of HO-1 and UGT1A1 and consequently the nuclear translocation of Nrf2, suggesting that a combination of low doses may be a promising strategy for cancer chemoprevention.

---

[1]Work described in this chapter is intended to be submitted for publication as: **Gomez, Y.**, Barve, A., Nair, S., Yu, S., Saw, C.L, and Kong, A.N.

[2]**Keywords**: curcumin, sulforaphane, combination treatment, HepG2C8 cells, Nrf2, antioxidant response element.

2.2 Introduction

There is a large body of evidence supporting an inverse relationship between the consumption of cruciferous vegetables and the incidence of several types of cancer including prostate cancer [60], lung cancer [61], bladder cancer [62], colon cancer [63], and pancreatic cancer [64]. Numerous studies have shown that phytochemicals in cruciferous vegetables up-regulate detoxifying enzyme systems such as phase II detoxifying enzymes, including NAD-(P)H: quinone reductase (NQO1), glutathione transferases (GSTs), UDP-glucoronosyl transferase (UGT), epoxide hydrolase , γ-glutamine cysteine synthetase (γ-GCS) as well as antioxidant enzyme systems such as heme oxygenase-1 (HO-1) [39, 65]. Furthermore, it has been demonstrated that regulation of the basal and inducible expression of these phase II detoxifying enzymes and antioxidant enzymes is mediated by the antioxidant response element (ARE), which is a cis-acting sequence found in the 5'-flanking region of genes encoding many phase II enzymes and antioxidant enzymes [66]. The ARE-mediated gene expression and therefore the induction of phase II/antioxidant enzymes have been linked to important protective mechanisms of cells/tissues against the toxic effects of reactive oxygen species (ROS), as well as endogenous or exogenous carcinogenic intermediates [67, 68]. Additionally, the coordinated induction of these phase II detoxifying enzymes is under the transcriptional control of the nuclear factor (erythroid-derived 2)-like 2 (NFE2L2 or Nrf2), a member of the cap 'n' collar (CNC) family of basic leucine zipper (bZIP), which is an essential component of the ARE-binding transcriptional machinery [34, 67]. Briefly, under normal basal conditions, Nrf2 is thethered to a cytosolic repressor protein called Kelch-like ECH-associated protein 1 (Keap1) [34]. The molecular cascades of ARE activation involves the dissociation of Nrf2 from Keap 1, followed by the

subsequent nuclear translocation of Nrf2, heterodimerization with small Maf (sMaf) protein, binding of the Nrf2/sMaf complex to ARE and ultimately initiation of the expression of ARE-driven genes [69].

Isothiocyanates (ITCs) are a chemical class of compounds generated from the metabolic biotransformation of naturally occurring cruciferous vegetables. This biotransformation is believed to occur by means of hydrolysis of secondary metabolites (glucosinolates) by the enzyme murosinase during the process of mastication or by the aid of resident microflora in the intestines, which promote the hydrolysis of glucosinolates into ITCs [26]. Sulforaphane (SFN; Fig. 2.1a), an isothiocyanate compound found in high levels in broccoli and broccoli sprouts, contributes to the induction of phase II detoxifying enzymes. Its high potency to inhibit tumorigenesis in animal models has been previously demonstrated. In the past, we reported that SFN results in the induction of hemeoxygenase-1 (HO-1) via activation of ARE and through the induction of Nrf2 protein in HepG2-C8 cells [34].

Curcumin (CUR; Fig. 2.1b), a yellow coloring constituent derived from the spice turmeric, has been shown to protect against many types of cancer and to suppress angiogenesis and metastasis in different animal models [24]. Moreover, the chemopreventive efficacy of CUR has been demonstrated through its ability to inhibit carcinogen bioactivation via suppression of specific cytochrome P450 enzymes or induction of phase II carcinogen detoxifying enzymes [70]. The precise mechanism of action is yet not fully elucidated, but literature suggests that mitochondrial hyperpolarization, resulting from ROS generation, is a prerequisite for CUR-induced apoptosis and the presence of mitochondrial DNA damage may be a probable mechanism for CUR to induce the apoptosis of HepG2 cells and serve as the initial event triggering a chain of events leading to cell death [71].

Since numerous dietary chemopreventive agents have shown anticarcinogenic activities when tested *in vitro* but have, nonetheless, failed to demonstrate a comparable efficacy *in vivo* or usually require non-readily achievable higher doses *in vivo*, it is of interest to test whether combination treatment involving lower doses of natural dietary agents that differ in their modes of action may be a more effective cancer chemopreventive strategy [72, 73].

The objectives of the present study were to investigate whether a combination treatment of low doses of SFN and CUR could modulate induction of antioxidant and phase II detoxifying enzymes such as HO-1 or UGT1A and to determine the nature of such interaction when tested in HepG2-C8 cells and to examine whether Nrf2 factor and ARE element are responsible for the mechanistic up-regulation of these antioxidant and phase II detoxifying enzymes.

2.3 Materials and Methods

2.3.1 Chemicals and Antibodies

CUR was obtained from Sigma (St Louis, MO). The purity of CUR was 70%. SFN was supplied by LKT laboratories (St Paul, MN) and its purity was > 99%. Luciferase Assay system was obtained from Promega (Madison, WI). Antibodies against HO-1, UGT1A, Nrf2, and β-actin were obtained from Santa Cruz Biotechnology Inc (Santa Cruz, CA). Trizol and SuperScript III first strand cDNA synthesis system were purchased from invitrogen (Carlsbad, CA). Cyclohexamide, an inhibitor of protein synthesis, and Actinomycin D, an RNA synthesis inhibitor, were purchased from Sigma Aldrich.

2.3.2 Cell Culture

HepG2-C8 cells generated in our laboratory by stable transfection of ARE-luciferase construct [74] were cultured and maintained in modified F-12 medium supplemented with 10 % FBS, 10 units/ml penicillin, 100 μg/ml streptomycin, 1% non-essential aminoacids, and 0.1 % insulin at

37 ^{o}C in a humidified incubator with 5% CO2. Cells were allowed to grow up for 24 hours to reach 70% confluency before replacing with modified F-12 medium containing 0.5% FBS for 12 h prior to treatment with CUR and SFN.

2.3.3 Western Blotting

HepG2-C8 cells were subjected to treatment with either CUR or SFN alone or to the combination of both agents (10 μM and 12.5 μM respectively). In the mechanistic investigation, 100 μg/ml of cyclohexamide was used. After treatments, cells were washed with ice-cold PBS (pH 7.4) containing 10 mM Tris-HCl, 50 mM sodium chloride, 30 mM sodium pyrophosphate, 50 mM sodium fluoride, 100 μM sodium orthovandate, 2 mM iodoacetic acid, 5 mM ZnCl2, 1mM phenylmethylsulfonyl fluoride, and 0.5% Triton-X 100. Cell lysates were vigorously vortexed, homogenized in an ultrasonicator for 10 sec and left on ice for 30 min. The homogenates were centrifuged at 13,000 rpm for 15 min at 4^{o}C. The supernatants were collected and equal amounts of total protein of each sample, as determined by BCA protein assay (Pierce, IL) were mixed with 4X loading buffer, and heated at 95 ^{o}C for 5 min. The samples were then separated in a 10 % criterion Tris-HCl precast gel at 200 V and transferred onto polyvinylidene difluoride (PVDF) membranes (Immobilion-P, Millipore, Bedford, MA) at 130 mA for 1.5 h using a semidry transfer system (Fisher, PA). The membranes were then blocked with 5% nonfat dry milk (1:5000 dilution) overnight at 4 ^{o}C. After hybridization with primary antibodies, membranes were washed three times with TBST (20 mM Tris-HCl, 8g/L NaCl, 0.1% Tween 20, pH 7.6) followed by incubation with anti-goat (for HO-1, UGT1A and β-actin) antibodies conjugated with horseraddish peroxidase (Santa Cruz Biotechnology Inc., CA) for 1 h at room temperature and washed again with TBST three times. Detection was performed using ECL

chemiluminescence reagent (Pierce, IL). Bands were visualized using Bio-Rad Imaging station. The protein expression was normalized against that of actin as a control.

2.3.4 RNA Extraction and Reverse Transcription-PCR (RT-PCR)

To further validate the western blotting results, we used semi-quantitative RT-PCR to examine the effects of CUR and SFN alone or both in combinations on the mRNA expression levels. HO-1, UGT1A1, and Nrf2 mRNA expression levels were evaluated using this technique. Actinomycin D (2 μg/ml) was used in the mechanistic investigation. Total RNA from HepG2-C8 cells were isolated by using a method of Trizol extraction coupled with the RNeasy kit from Qiagen (Valencia, CA). RNA integrity was examined by electrophoresis and concentrations were determined by UV spectroscopy (DU 530 Life Science UV/Visible spectrophotometer, Fullerton, CA). Total RNA was then reverse transcribed to single-stranded cDNA by the SuperScript III first-strand cDNA synthesis system. The specific primers for HO-1 and β-actin genes were designed by using Primer Express 2.0 software (Applied Biosystems, Foster City, CA). The 5' and 3' primers used for amplifying HO-1 were 5'GGT GAC CCG AGA GGG CTT-3' and 5'-CGA AGA CTG GGC TCT CCT TGT-3'. β-actin was used as an internal control and was amplified with the 5' and 3' primers: 5'-CAG TGT GGG TGA CCC CGT-3' and 5'-CCC AGC CAT GTA CGT TGC TA-3'. The HO-1 gene expression levels were analyzed by normalization with control β-actin levels. The 5' and 3' primers used for amplifying UGT1A were 5'-TAA GTG GCT ACC CCA AAA CG-3' and 5'-TCT TGG ATT TGT GGG CTT TC-3'. The 5' and 3' primers used for amplifying Nrf2 were 5'-TGA AGC TCA GCT CGC ATT GAT CC-3' and 5'-AAG ATA CAA GGT GCT GAG CCG CC-3'. PCR conditions were as follows: 94 ^{o}C for 5 min followed by 40 cycles of denaturation at 94 ^{o}C for 30 s, annealing at 55 ^{o}C for 45 s, extension at 72 ^{o}C for 1 min, and a final extension at 72 ^{o}C for 10 min.

2.3.5 Luciferase Reporter Assay

The ARE-luciferase activities in HepG2-C8 cells were determined using a Luciferase assay system according to the manufacturer's instructions. Briefly, after treatment, cells in six-well plates were washed twice with ice-cold phosphate-buffered saline (PBS; pH 7.4) and were lysed by adding 400 μl of 1X reporter lysis buffer (Promega, CA After centrifugation at 12,000 x g for 15 s at room temperature, 10 μl aliquot of supernatant was analyzed for luciferase activity by reading with a SIRIUS luminometer (Berthold Detection System, Germany). Normalization of the luciferase activity was done based on the protein concentration, which was determined by using BCA protein assay kit from Pierce Biotechnology (Rockford, IL). The luciferase activity was then expressed as fold of induction over the activity of control vehicle-treated cells. Several SFN/CUR dose combinations were tested (2.5/2.5, 5/2.5, 12.5/2.5, 1/1, 1/0.5 and 12.5/10(μM)). Values are expressed as $\pm$ SD of experiments and all experiments were done in triplicate.

2.4 Results

2.4.1 Individual Doses of Curcumin and Sulforaphane can Induce HO-1 Enzyme

The ability of SFN or CUR to induce the HO-1 protein expression level at different dose concentrations in HepG2-C8 cells after exposure for 6 h was evaluated by western blotting (Fig. 2.2a and 2.2b). Both SFN and CUR resulted in a dose-dependent induction of the HO-1 protein except for SFN concentrations equal or higher than 20 μM and CUR concentration above 10 μM. Protein levels were normalized to β-actin. Maximal CUR or SFN-mediated HO-1enzyme induction was seen at a concentration of 10 μM or 12.5 μM respectively. Our findings were further confirmed by RT-PCR. The HO-1 mRNA level as well as the UGT1A1 mRNA level were measured after pre-treating the HepG2C8 cells with the same concentrations of CUR or

SFN that were used in the western blotting experiments (Fig. 2.2a and 2.2b) for 6 h. As evidenced in Fig. 2.2c, the results obtained for HO-1 mRNA expression by RT-PCR were in agreement with the results obtained by western blotting analysis, while the mRNA expression of UGT1A1 remained similar to the basal expression. Based on the latter results and because concentrations of CUR above 10 μM have previously been shown to be highly toxic [75] , we chose to study the combinatorial effects of 12.5 μM of SFN and 10 μM of CUR, thus ensuring cotreatment with concentrations below toxic levels.

2.4.2 The Combination Therapy of Curcumin and Sulforaphane Results in Greater Induction of HO-1 Enzyme

In order to investigate the chemopreventive effects of the combination treatment of SFN (12.5 μM) and CUR (10 μM) on the induction of both antioxidant and phase II detoxifying enzymes in HepG2-C8 cells, we performed analysis of target HO-1 and UGT1A1 proteins with specific antibodies by western blotting after pre-treatment of HepG2-C8 cells with SFN (12.5 μM), CUR (10 μM) or the combination of both agents as shown in Fig 2.3a. Interestingly, the potency of CUR to induce such antioxidant and phase II enzymes was less than that of SFN in agreement with previous studies [34, 68] and the potency of the combination therapy was markedly higher, especially for the HO-1 protein induction. To further confirm these results, we investigated the expression levels of these two antioxidant and phase II detoxyfying enzymes after 6 h of pretreatment of HepG2-C8 cells with individual doses of SFN (12.5 μM) and CUR (10 μM) or with their combined doses by RT-PCR (Fig. 2.3b). The combined effect of SFN and CUR was markedly higher compared with expression levels of both proteins by individual doses of each phytochemical alone.

2.4.3 Transcriptional Induction of Nrf2-mediated Gene Expression by the Combination of Sulforaphane and Curcumin is Dependent on *de novo* Synthesis

To determine whether the transcriptional activation of the UGT1A1 and HO-1 genes might require de novo protein synthesis, we incubated HepG2-C8 cells for 6 h with the combination therapy of Cur (10 μM) and SFN (12.5 μM) in parallel with each single dose and in the presence of 100 μg/ml of cyclohexamide, an inhibitor of protein synthesis (Fig. 2.3c). In the presence of cyclohexamide, the induction of the HO-1 as well as UGT1A1 genes by the combination therapy was markedly down-regulated after treatment with the dual combination of agents. These results provide evidence that *de novo* protein synthesis is required for expression of both HO-1 and UGT1A genes induced by CUR and SFN.

2.4.4 Effect of the Combination Therapy on Nrf2-mediated mRNA Stability

We next examined whether stimulation with the combination treatment was confined to induction of transcription only. We simultaneously pre-treated HepG2-C8 cells with SFN (12.5 μM), CUR (10 μM) or their combination with Actinomycin D (2 μg/ml), an RNA synthesis inhibitor, for 6 h. The mRNA gene expression level was measured after 6 h of co-treatment. The same experiment was performed in cultures treated with single doses of each individual chemopreventive agent as well as with vehicles alone as controls. The effects in HO-1 and UGT1A1 mRNA levels after inhibition of RNA synthesis was measured by RT-PCR (Fig. 2.3d). Co-treatment with SFN (12.5 μM) and actinomycin D or CUR (10 μM) and actinomycin D did not cause an apparent HO-1 mRNA expression difference as compared with the same treatment without the inhibitor (Fig. 2.3b). Indeed, the HO-1 mRNA expression levels remained similar as without treatment with actinomycin D. Very interestingly, however, stimulation of the HO-1 mRNA level by the combination treatment of CUR and SFN was dramatically abrogated by

actinomycin D, remaining below basal levels. On the other hand, actinomycin D reduced the UGT1A1 mRNA expression level after stimulation of the HepG2-C8 cells by single treatment of CUR or SFN as well as after treatment with the combined therapy (Fig. 2.3d) in comparison with results obtained in Fig. 2.3b. However, the mRNA expression of UGT1A remained above basal levels.

Taken together, these results suggest that the combination of CUR and SFN may transcriptionally regulate the expression of HO-1. While the exact mechanism by which they regulate UGT1A1 is currently unknown, it is speculated that they effect translational regulation of UGT1A1. However only detailed biochemical assays may help to delineate the exact mechanism of induction by CUR and SFN.

2.4.5 The Combination of Curcumin and Sulforaphane is Mediated Through Nrf2 Activation

Nrf2 is an oxidant-responsive transcription factor that has previously been shown to modulate CUR-mediated induction of HO-1 [75] and to play a critical role in SFN-mediated induction of HO-1 [34]. We investigated whether the combination of CUR (10 μM) and SFN (12.5 μM) was able to up-regulate the mRNA expression level of the Nrf2 factor. First, we tested the ability of each drug alone to induce the Nrf2 transcription factor in HepG2-C8 cells at different doses and after a 6 h pretreatment. As indicated in Fig. 2.4a, both SFN and CUR were able to up-regulate the mRNA level of the Nrf2 transcription factor exhibiting a maximal expression for 12.5 μM of SFN or 10 μM of CUR. We, then, tested the effect of the combination treatment of CUR (10μM) and SFN (12.5 μM) on the expression of the Nrf2 factor in whole cell lysates (Fig. 2.4b). We found that the combination therapy exhibited a greater inductive effect on the Nrf2 mRNA expression level than each dose alone. These results indicated that, in HepG2-C8 cells, the

induction of the HO-1 and UGT1A1 by the combination treatment of SFN and CUR is due to the activation of the ARE-driven gene expression via up-regulation of Nrf2.

2.4.6 Nuclear Translocation of Nrf2 by the Combination Therapy of Curcumin and Sulforaphane

To investigate the nature (whether cytoplasmic or nuclear) of Nrf2 induction by the combination treatment of CUR (10 μM) and SFN (12.5 μM), both the cytoplasmic extract and the nuclear extract from HepG2-C8 cells after a 6 h pretreatment were assayed for expression of Nrf2 by RT-PCR. Fig. 2.4c clearly shows that the level of Nrf2 mRNA expression in the cytoplasmic extract was less than the nuclear level for both treatments with single doses of each chemopreventive agent alone or the combination of SFN and CUR. Additionally, the level of endogenous Nrf2 mRNA expression was more strongly induced in the nuclear extract for all the treatments with a markedly over-expressed induction seen for the combination treatment.

2.4.7 Combination of CUR and SFN Synergistically Activate ARE Luciferase Reporter Gene Activity in HepG2C8 Cells

To determine the chemopreventive effect of the combination treatment of CUR and SFN on the ARE-mediated gene expression, the ARE-luciferase activity elicited by this combination of agents was evaluated in HepG2-C8 cell line [74]. As shown in Fig. 2.5a and 2.5b, treatment with CUR alone resulted in a maximal induction of around 5-fold over control and treatment with SFN exhibited a maximal induction of around 18-20 fold over control. We were interested in testing the combination of low doses (10 μM of CUR and 12.5 μM of SFN) of these agents to determine potential enhancement in the ARE luciferase activity. As can be seen in Fig. 2.5c, 10 μM of CUR resulted in around 2-fold induction, 12.5 μM of SFN resulted in around 8 to 9-fold induction whereas the combination treatment exhibited a significant (p-value <0.05) synergestic

induction of the ARE luciferase activity of around 16-fold. In order to determine the potential synergetic interaction of lower doses of the combination of these two agents in the ARE-luciferase activity, we performed isobologram analysis as reported by Zhao et al [76]. Briefly, the CUR/SFN combinations tested were: 2.5/2.5, 5/2.5, 12.5/2.5, 1/1, 1/0.5 (μM). All these combinations of lower doses exhibited a synergestic induction as shown by the isobologram in Fig. 2.5d. Furthermore, the corresponding combination indices were less than 1 (data not shown) which further confirmed the synergestic effect of combination therapies of low doses of the dietary phytochemicals CUR and SFN.

2.5 Discussion

SFN is part of the ITC family of compounds and has been investigated to a great extent. Furthermore, it has been proven to be a potent inducer of phase II detoxifying and antioxidant enzymes including NQO1, HO-1, and glutathione S-transferases [34, 77]. Additionally, several studies have implicated SFN as a main activator of the ARE-driven enzyme expression via activation of the Nrf2 transcription factor [34]. CUR is another well studied chemopreventive agent that has shown great efficacy in providing cytoprotective properties via induction of antioxidant enzymes including HO-1 and through activation of the Nrf2 transcription factor [75]. It is well known that induction of these Nrf2-mediated enzymes regulates important biological mechanisms that ultimately provide protection against toxicological effects arising from exogenous carcinogens or endogenous reactive oxygen species. This induction is mainly regulated by the ARE promoter regions of the genes [78, 79].

Despite the significant *in-vitro* anticarcinogenic effects provided by dietary phytochemicals, *in-vivo* studies have revealed that they need to be administered in high doses that may not be readily bioavailable to physiological systems and that in turn can cause greater toxicity in the

experimental models [72, 73]. As a result, there is an increasing need to investigate the potential benefits of combination of low-dose drug regimes, preferentially those that exert their mechanistic mode of action by targeting different molecular pathways, as this methodology can result in improved therapeutic benefits while augmenting efficacy and reducing toxicity [80]. Previously, our lab has demonstrated synergestic transcriptional activation of the AP-1 reporter gene in HT-29 cells by the combination of SFN and (-) Epigallocatechin-3-gallate (EGCG) dietary factors [53]. Additionally, we demonstrated that the combination of CUR and phenylethyl isothiocyanate (PEITC) was more effective in suppressing prostate adenocarcinoma in the TRAMP mouse model [81]. Given the abundance of literature on the multiple anti-carcinogenic mechanisms of SFN and CUR, this study was aimed at examining the effects of the combination therapy of low doses of CUR and SFN in both the expression of the HO-1 antioxidant and the UGT1A1 phase II detoxifying enzymes as well as in the ARE-luciferase activity and was focused on investigating whether the Nrf2 transcription factor was involved in the ARE-driven expression of such enzymes in HepG2-C8 cells.

We investigated the ability of individual treatments of SFN or CUR to induce protein expression of HO-1 as well as the efficacy of the combinatorial treatment. HO-1 is a stress responsive enzyme and a natural mechanism of cellular defense. HO-1 induction is a complex multi-regulated process involving multiple transcription factors and is readily upregulated in response to intracellular oxidative stress [75]. Indeed, the combination treatment resulted in a stronger induction of this important antioxidant enzyme compared with treatment with the individual agents. This observation correlated well with the mRNA expression levels of HO-1 obtained by RT-PCR. Furthermore, the induction of the protein and mRNA expression levels of UGT1A1 by the combination treatment of SFN and CUR was also investigated. Our results indicated that

UGT1A1 protein level was more strongly induced by the combination treatment than by each individual compound alone. This result was in agreement with the mRNA expression level. We also showed that the transcriptional induction of these two important ARE-mediated enzymes by the combinatorial effects of SFN and CUR is dependent on *de novo* protein synthesis as demonstrated by the abrogation of the HO-1 and downregulation of the UGT1A1 proteins by the protein synthesis inhibitor, cyclohexamide. Furthermore, co-treatment of HepG2-C8 cells with the combination treatment and the RNA synthesis inhibitor actinomycin D, indicated that regulation of the HO-1 mRNA induction does not occur through mRNA stabilization, but the regulation of UGT1A1 may be controlled via mRNA stabilization as inferred by the facts that the combination therapy- mediated induction of HO-1 mRNA expression level was fully attenuated by the RNA inhibitor whereas the combination therapy-mediated induction of UGT1A1 mRNA expression level remained the above control levels after inhibition with actinomycin D.

There are many potential mechanisms through which CUR may induce HO-1 expression including ROS generation, Nrf2 activation and kinase activation [75]. On the other hand, studies on the chemopreventive mechanism of SFN-mediated induction of HO-1 in HepG2 human hepatoma cells suggests that this process occurs through Nrf2 induction, as a consequence of its retarded degradation through Keap1 inhibition, and ARE-mediated transcription activation [67]. In order to elucidate if the molecular mechanism by which the combination treatment of CUR and SFN induce such ARE-mediated enzymes, including HO-1 and UGT1A, is through Nrf2 transcriptional activation, we measured the mRNA levels of Nrf2 in HepG2-C8 cells after treatment with the combination of both chemopreventive agents. Our results indicated that the mRNA expression level of Nrf2 was up-regulated following treatment with the combined agents. It is also evident that this up-regulation is higher for the combination therapy than for single

compounds. Furthermore, to address whether Nrf2 induction by the combination treatment occurred at the cytoplasmic or nuclear levels, we measured the mRNA Nrf2 expression levels of both the cytoplasmic and nuclear extracts. Our results revealed that, indeed, induction of the Nrf2 factor by the single agents or the combination occurred at the nuclear level with a dramatic over-expression seen for the combination treatment. It is possible that nuclear accumulation of Nrf2 might be facilitated by suppressing Keap1 activity. However, this possibility remains yet to be studied.

Since regulation of the basal and inducible expression of antioxidant phase II detoxifying enzymes has been shown to be mediated by ARE and because coordinated induction of these enzymes is regulated by Nrf2 [66, 67], we were interested in evaluating the nature of action of the combination treatment on the ARE-luciferase expression of HepG2-C8 cells. Using isobologram analysis and combination indices as described by Zhao, et al. [76], we found that combination of low doses of these two chemopreventive agents exhibited a significant synergestic induction on the ARE luciferase activity.

Taken together, these results suggest that SFN when combined with CUR at low doses exhibit an enhanced ability to induce important phase II detoxifying and antioxidant enzymes both at the protein and mRNA levels. The mechanism for this induction is mediated by the concerted action of Nrf2/ARE up-regulation. When the combination treatment is not administered in toxic doses, it results in synergestic induction of the ARE-antioxidant mediated activation. Combination of low doses of chemopreventive agents may therefore be an important strategy for the prevention and management of several types of cancer.

Since regulation of the basal and inducible expression of antioxidant phase II detoxifying enzymes has been shown to be mediated by ARE and because coordinated induction of these

enzymes is regulated by Nrf2 [66, 67], we were interested in evaluating the nature of action of the combination treatment on the ARE-luciferase expression of HepG2-C8 cells. Using isobologram analysis and combination indices as described by Zhao, et al. [76], we found that combination of low doses of these two chemopreventive agents exhibited a significant synergestic induction on the ARE luciferase activity.

Taken together, these results suggest that SFN when combined with CUR at low doses exhibit an enhanced ability to induce important phase II detoxifying and antioxidant enzymes both at the protein and mRNA levels. The mechanism for this induction is mediated by the concerted action of Nrf2/ARE up-regulation. When the combination treatment is not administered in toxic doses, it results in synergestic induction of the ARE-antioxidant mediated activation. Combination of low doses of chemopreventive agents may therefore be an important strategy for the prevention and management of several types of cancer.

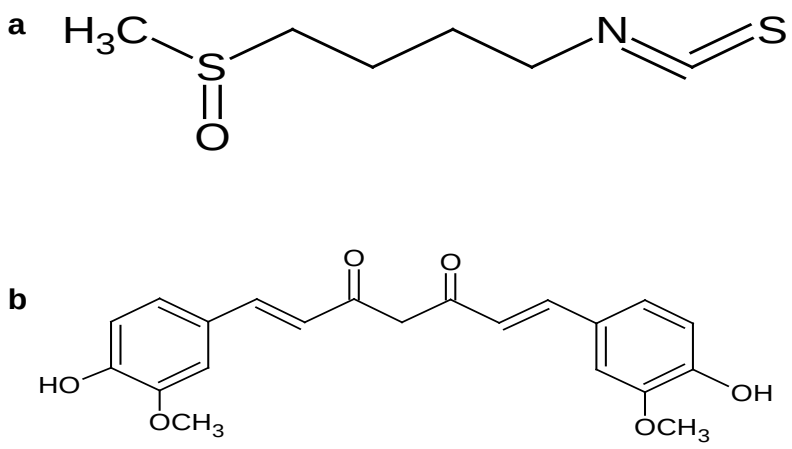

Fig. 2.1 Chemical Structures of chemopreventive agents used in this study. (**a**) Sulforaphane (**b**) Curcumin

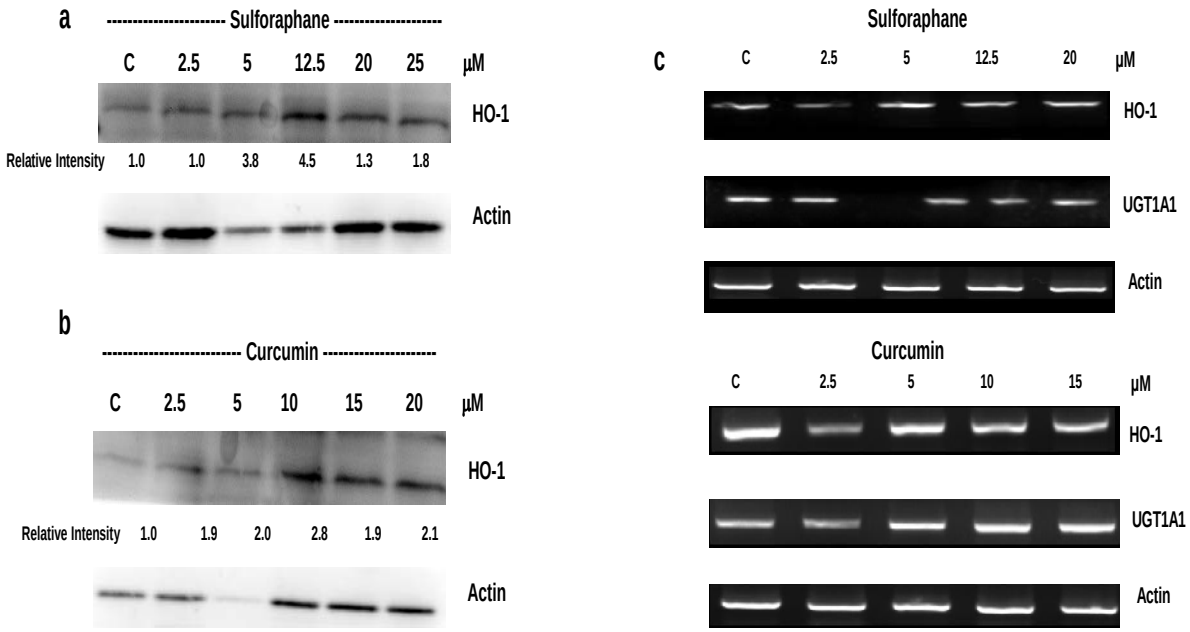

Fig. 2.2 Effects of individual doses of chemopreventive agents (CUR and SFN) on the induction of antioxidant enzymes. **(a)** The ability of SFN to induce the HO-1 protein expression level at different dose concentrations in HepG2-C8 cells after 6 h of exposure was assessed by western blotting. **(b)** HO-1 protein induction by CUR was assessed by western blotting after 6 h of exposure of HepG2-C8 cells to this phytochemical; actin was used to ensure equal protein loading. **(c)** Induction of HO-1 and UGT1A1 at the mRNA level was measured by RT-PCR after exposure of HepG2-C8 cells to different dose concentrations of CUR or SFN for 6 h. C: control (0.2% DMSO).

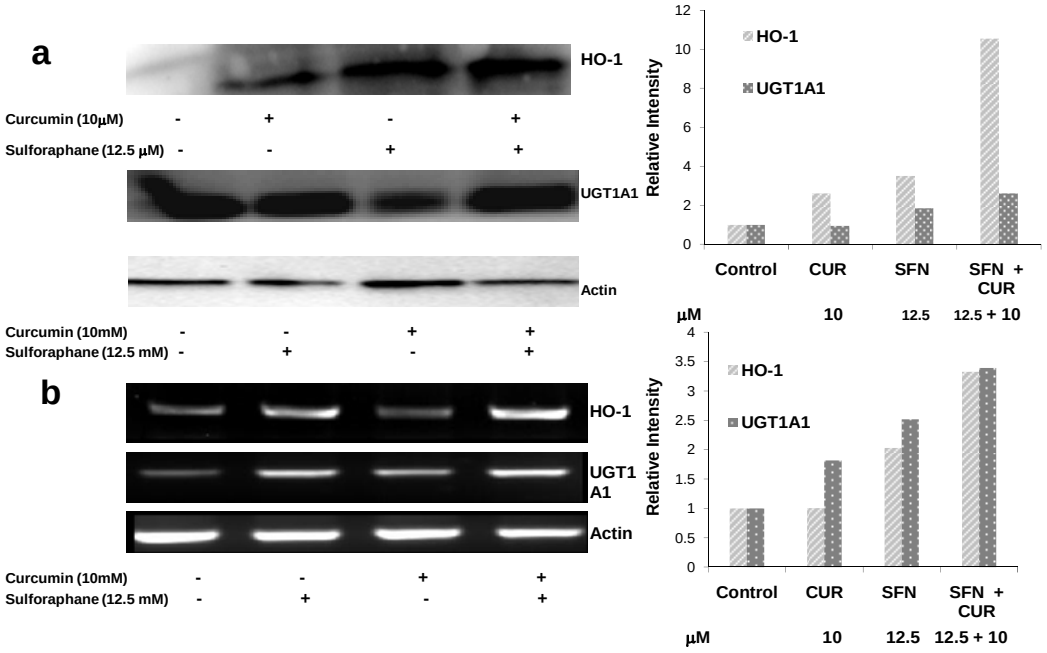

Fig. 2.3 Effects of the combination therapy of CUR and SFN on the induction of HO-1 and UGT1A1 both at the protein and mRNA levels. **(a)** HepG2-C8 cells were treated with CUR (10μM), SFN (12.5 μM), or the combination of both agents (10 μM CUR + 12.5 μM SFN) for 6 h. The protein level of HO-1 and UGT1A1 was assessed by western blotting and normalized to actin. **(b)** The mRNA expression level of antioxidant and phase II genes was evaluated by RT-PCR. mRNA was extracted 6 h after treatments and HO-1 and UGT1A1 levels were measured. The mRNA level of HO-1 and UGT1A1 was assessed by PCR and normalized to actin.

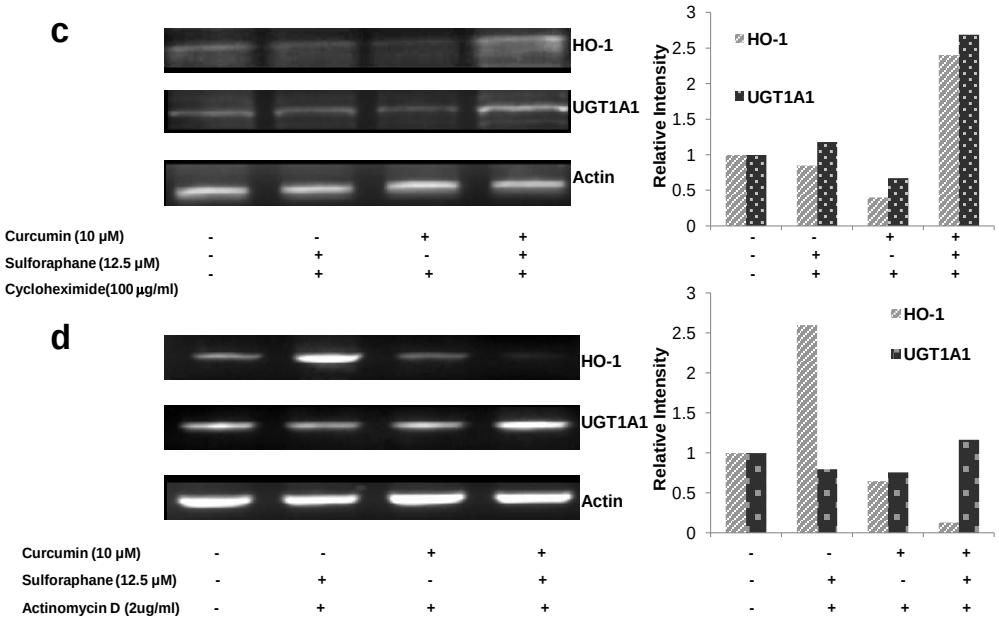

Fig. 2.3 (Cont'd) Effects of the combination therapy of CUR and SFN on the induction of HO-1 and UGT1A1 both at the protein and mRNA levels. **(c)** The induction of HO-1 and UGT1A1 genes requires *de novo* protein synthesis according to results obtained by protein inhibition with cyclohexamide, compared with Fig. 3 (a). The protein level of HO-1 and UGT1A1 was assessed by western blotting and normalized to actin. **(d)** Regulation of HO-1 mRNA by the combination therapy does not happen by mRNA stabilization, but the regulation of UGT1A1 may be controlled by mRNA stabilization. The mRNA level of HO-1 and UGT1A1 was assessed by PCR and normalized to actin.

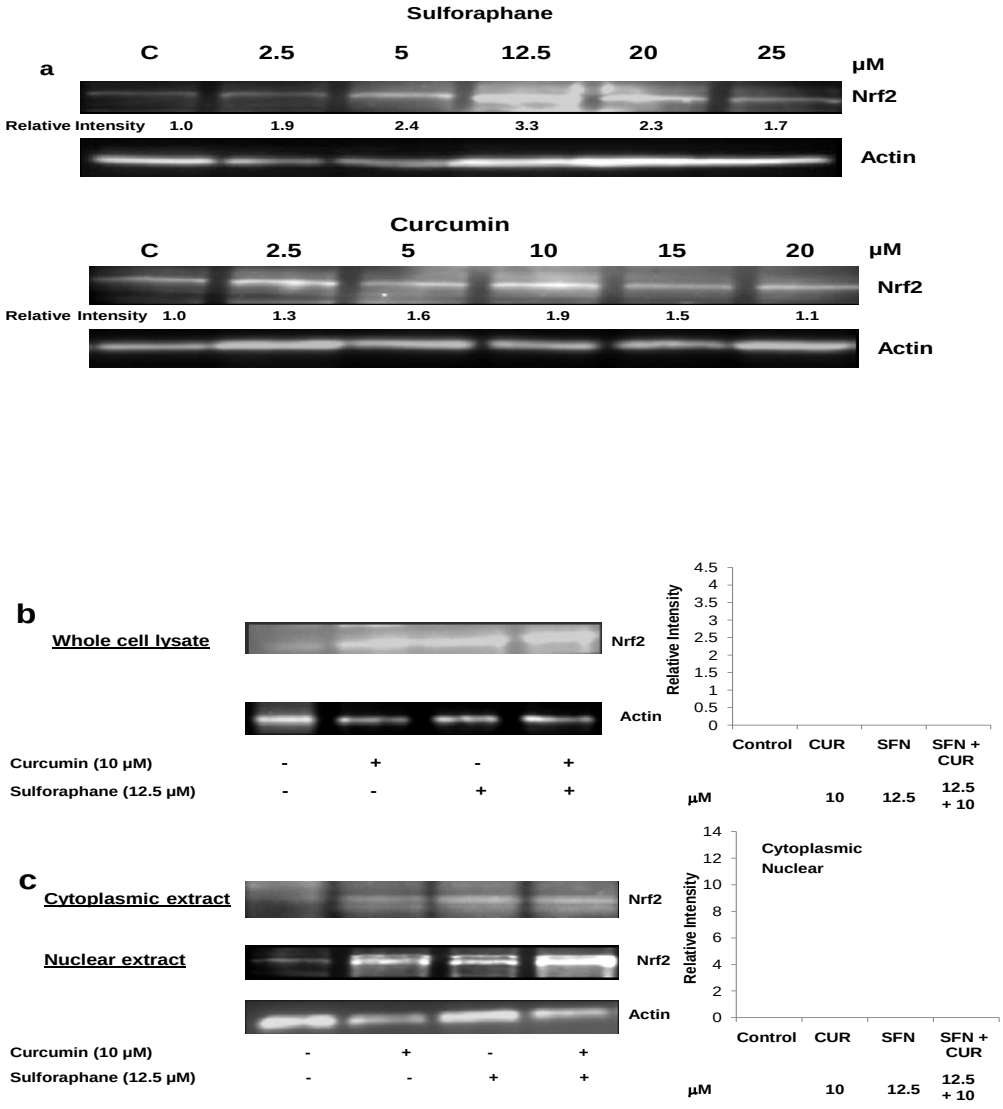

Fig. 2.4 The ability of the combination therapy to induce Nrf2 mRNA expression was assessed by RT-PCR after incubation of the HepG2-C8 cells with both agents for 6 h. **(a)** The ability of each individual chemopreventive agent to up-regulate the Nrf2 genotypic expression at different dose concentrations was assessed. **(b)** Whole cell lysate: The efficacy of the combination therapy (CUR 10 μM + SFN 12.5 μM) to induce Nrf2 mRNA expression was evaluated. The mRNA level of Nrf2 was assessed by PCR and normalized to actin. **(c)** Cytoplasmic and nuclear extract: in order to determine the nature of Nrf2 induction (whether cytoplasmic or nuclear), the mRNA level was measured for both the cytoplasmic and nuclear extracts. The mRNA level of Nrf2 was assessed by PCR and normalized to actin. The level of Nrf2 in the nuclear extract is higher than the cytoplasmic level, indicating Nrf2 nuclear translocation. C: control (0.2% DMSO).

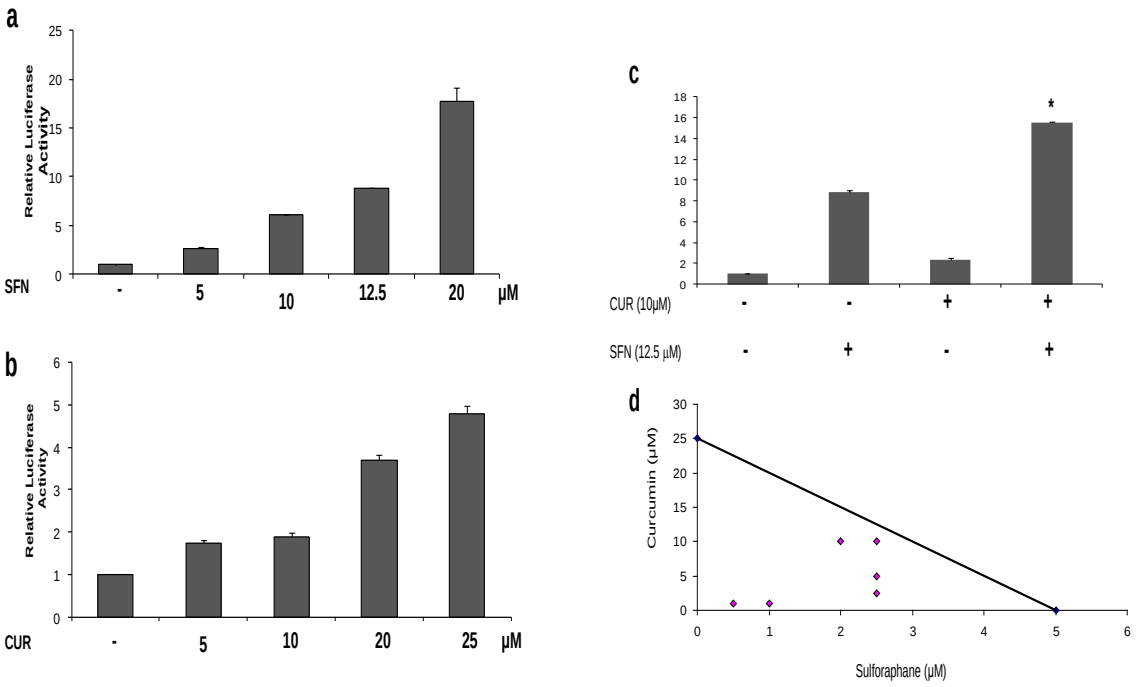

Fig. 2.5 Combined effects of CUR and SFN on the ARE-luciferase activity of HepG2-C8 cells. Data are shown as ± SD (n = 3). For t-tests * $p < 0.05$ compared with treatments by single agents. **(a, b)** The ARE-luciferase activity was measured after pre-treatment of HepG2-C8 cells with different dose concentrations of the individual chemopreventive agents: CUR or SFN for 24 h. **(c)** The ARE-luciferase activity after exposure of HepG2-C8 cells for 24 h to the combination therapy of CUR (10 μM) and SFN (12.5 μM) was measured. The nature of interactions (i.e. synergestic, additive, or antagonistic) for several combinations of low doses of dietary factors CUR and SFN was assessed by the isobologram method analysis as described elsewhere [76]. Briefly, combination therapies of SFN/CUR were 0.5/1; 1/1; 2/12.5; 2.5/2.5; 2.5/12/5. Data points are described by concentrations (in μM) of SFN and CUR reflected on *x*- and *y*- axis respectively, and are representative of three independent experiments. The corresponding combination indices were less than 1.0 (data not shown) which further confirmed the synergestic effect of combination therapies of low doses of the dietary phytochemicals CUR and SFN.

CHAPTER 3

Development and Validation of a Rapid UPLC/MS Method for the Simultaneous Determination of I3C, DIM, and Related Metabolites and its Application to Pharmacokinetics in Rats[3,4,5,6]

3.1 Abstract

Indole-3-Carbinol (I3C) and Diindolylmethane (DIM) are naturally derived phytochemicals with promising anticarcinogenic properties previously demonstrated both in-vitro and in-vivo. Using reversed-phase ultra performance liquid chromatography (UPLC) coupled with mass spectrophotometry (MS), a rapid, specific, and high throughput method was developed and validated for the quantification and identification of I3C, DIM, and other I3C metabolites in plasma. Samples containing I3C or DIM and the internal standard 4-Methoxy indole (IS) were extracted using protein precipitation technique. The mean recovery was 96.21 % for I3C and 108.5% for DIM. Separation was achieved using a Waters Acquity UPLC HSS T3, 1.8 μm 2.1 x 150 mm column and acetonitrile/water gradient elution. The flow rate was 0.3 mL/min and the run time was 9 minutes. The limits of detection and quantification for both I3C and DIM were 10 ng/mL and 25 ng/mL respectively. Calibration curves of I3C and DIM were linear ($r > 0.99$) over a concentration of 0.025 – 20 μg/mL. Precision, accuracy, and stability analysis fulfilled the criteria of the CDER guidelines. The method was successfully applied to the determination of the pharmacokinetic parameters of I3C or DIM after oral, intravenous, or intraperitoneal administration to Sprague Dawley rats. The method described here was optimized over existing analytical methods for I3C and its metabolites in terms of sensitivity, speed, and separation.

[3]Work described in this chapter is intended to be submitted for publication as: **Gomez, Y.**, Wang, H., and Kong, A.N.

[4]UPLC/MS instruments and WinNonlin Software were provided by McNeil Consumer Healthcare (a Johnson & Johnson family of companies; Fort Washington, PA)

[5]**Keywords:** UPLC/MS; Indole-3-Carbinol; Diindolylmethane; Pharmacokinetics; single-dose administration; Sprague-Dawley Rats

[6]**Abbreviations:** I3C, indole-3-Carbinol; DIM, 3,3-diindolylmethane; IS, 4-methoxy indole; I3CA, indole-3-carboxylic acid; I3A, indole-3-carboxaldehyde; DIMOH, di-1H-indol-3-ylmethanol; DIM, 3,3-diindolylmethane; DIMO, di-1 H-indol-3-ylmethanone; HI-IM, [1-(3-hydroxymethyl)-indolyl-3-indolylmethane; ICZO, indole-[3,2*b*]-carbazole-6,12-(5*H*,11*H*)-dione; LTr1, linear trimer [2-(indol-3-ylmethyl)-indol-3-yl]indol-3-ylmethane; CTr, cyclic trimer 5,6,11,12,17,18-hexahydrocyclonona[1,2-b':4,5-b9:7,8-b'']tri-indole.

3.2 Introduction

There is abundant literature supporting the fact that undertaking a healthy diet rich in fruits and vegetables help reduce or prevent the incidence of carcinogenesis [82-85]. The incidence of prostate cancer was shown to be minimized in individuals who consumed high amounts of cruciferous vegetables [84]. Among the many naturally-derived components with anticarcinogenic properties are Indole-3-Carbinol (I3C) and its condensation product 3,3-Diindolylmethane (DIM). Several studies have revealed the marked modulatory ability of condensation products of I3C on xenobiotic and estrogen metabolism for the prevention of breast cancer [86, 87]. Prevention of cervical cancer by I3C may also be linked to its antiestrogenic effects in cervical cancer cells [88]. Furthermore, studies in several animal models have indicated that I3C can block hormone or chemical-induced carcinogenesis in different mammal species or fish. However, it can also favor carcinogenesis under some experimental conditions [89-93]. Due to the rapid formation of DIM after the acid-mediated polymerization of I3C in the low pH environment of the gastrointestinal tract, it is believed that DIM may be responsible for eliciting the anticarcinogenic pharmacological effects after oral administration of I3C [94, 95]. In fact, DIM has been shown to induce apoptosis in human PC3 prostate cancer cells via the mitochondrial pathway as evidenced by the increase in caspase activity and cytochrome *c* release into the cytosol [96]. Studies in rodents have also revealed DIM antiestrogenic potential against cancer elicited via a blockade of the aryl hydrocarbon/ estrogen receptor pathways [97].

To date, a couple of high performance liquid chromatography (HPLC) methods have been developed [50, 98] for the analysis of I3C and its metabolites in plasma and tissue of rodents [48, 49] and humans [50, 51]. However, only one method has been validated [98] . Furthermore, such validated method requires a run time of 60 minutes and has a quantification limit 50 ng for both

I3C and DIM, which pose a significant limitation in terms of both the analytical throughput and sensitivity of the method. This article describes, for the first time, the development and validation of a specific, sensitive, and reproducible UPLC/MS method for the rapid quantification and identification of I3C and its metabolites including DIM in rat plasma. This is the first chromatographic method with more than six-fold improvement in run time and two-fold improvement in sensitivity.

Several studies have investigated the biological fate of I3C upon oral administration and all have shown that I3C undergoes significant metabolism into several oligomerization products to such an extent that in less than an hour I3C falls below the limit of quantification [48, 50]. Furthermore, there is a lack of literature on the pharmacokinetics of I3C following alternate routes of administration. Therefore, in the present study, the validated method was successfully applied to the evaluation of the pharmacokinetic parameters in Sprague Dawley rats following administration of I3C via intravenous (i.v.) or intraperitoneal (i.p.) routes using two different delivery vehicles, and after administration of a promising polymeric DIM formulation via i.v. or oral (p.o.) routes.

3.3 Experimental Methods

3.3.1 Chemicals and Supplies

Indole-3-Carbinol (I3C), 3,3-Diindolylmethane (DIM), internal standard 4-Methoxy Indole (IS) (Figure 3.1), Tris base, ethanol (99 %) and Diisopropyl Ether (98%) were purchased from Sigma Aldrich (St. Louis, MO). Ammonium Formate, Formic Acid, DMSO, and Acetonitrile (HPLC grade) were purchased from JT Bakers (Phillipsburg, NJ). De-ionized water was obtained from a MilliQ System (Millipore, Bedford, MA). Heparin Sodium Injection, USP (1000 U/mL) and Sodium Chloride Injection, USP (0.9%) were obtained from Baxter Healthcare Corporation

(Deerfield, IL), and Hospira Inc (Lake Forest, IL) respectively. Spin X Centrifuge tube filters, 0.22 μm and HPLC limited volume vials were purchased from VWR International (West Chester, PA).

3.3.2 Animal Studies

Male Sprague-Dawley rats bearing jugular vein or portal vein-cannulae and weighing 200 to 300 g were purchased from Hilltop Laboratories (Scottsdale, PA). The animals were kept at the Animal Care Facility at Rutgers University and allowed free access to food and water during a three day acclimatization period (12 hour dark-light cycles) after which they were fed an antioxidant-free AIN-76A diet (Dyets Inc, PA) for 2-3 days prior to commencing the studies. All animal procedures were performed in accordance with Institutional Animal Care and Use Committee guidelines and approved protocols were followed. On the day of the study, the cannulae was exteriorized and connected to polyethylene tubing (Instech Laboratories, PA) wrapped in wire coils for blood collection. Heparinized Saline (50 U/mL) was used to flush the cannulae. Rats were fasted overnight prior to administration of I3C or DIM doses. 100 mg/kg of I3C was intraperitoneally (i.p.) administered to rats (n = 4) in a vehicle composition of Cremaphor/Tween-80/PEG 400/Ethanol/ water (2:1:1:1:5). Another group of rats (n = 4) received 25 mg/kg of I3C in a same vehicle composition, as an intravenous (i.v.) bolus through the jugular vein cannulae. Additionally, 50 mg/kg of I3C was administered i.p. to rats (n = 6) in a vehicle composition of DMSO and olive oil (1:4 v/v). Animals were used for a cross-over study of DIM after a one-week wash out period. Rats (n = 4) received a 20 mg/kg i.v. dose of DIM suspended in a vehicle composition of Cremaphor/Tween-80/PEG 400/Ethanol/ water (2:1:1:1:5) via the jugular vein cannulae. Similarly, a DIM oral dose of 200 mg/kg suspended in a similar vehicle composition was administered by oral gavage (n =4). The dosing regimens for I3C and

DIM were based on previous studies in rodents [48] where oral administration of 250 mg/kg of I3C was well tolerated and also based on the established conception that such dose would provide a concentration intake higher than normally consumed in a normal diet [48]. Since intraperitoneal administration partly bypasses fist pass metabolism, I3C i.p. doses in this study were chosen to be lower than p.o. doses in [48] in order to diminish or eliminate potential toxic effects. Blood samples (0.3 mL) were withdrawn at regular time intervals up to 12-24 hours into heparinized vials, followed by replacement with an equal volume of saline. All blood samples were immediately centrifuged at 2500 rpm to obtain plasma samples and stored at -20 ^{o}C until analysis.

3.3.3 Preparation of Standards and Quality Control Samples

Primary stock solutions of I3C (4 mg/ml), DIM (4 mg/ml), and IS (1 mg/ml) were prepared in DMSO and stored at – 80 ^{o}C. Primary stock solutions were serially diluted in ACN:25 mM Tris buffer (50:50 v/v) to prepare working solutions with concentrations of 0.25, 0.5, 1.0, 2.5, 5.0, 10, 50, 100, and 200 μg/ml for the calibration curves or 0.25 (low), 50 (medium), and 150 (high) μg/ml for the quality control (QC) samples. The primary stock solution of IS was diluted to a final concentration of 0.4 mg/ml in the same diluent composition described above. Working solutions were stable at -20 ^{o}C for at least 1 month. Calibration curve samples (0.025, 0.05, 0.1, 0.25, 0.50, 1.0, 5.0, 10, and 20 μg/ml) and QC samples (0.25, 5.0, and 15 μg/ml) were prepared fresh daily by spiking 50 μl of plasma with 5 μl of ACN: 25mM Tris (50:50 v/v) for blank standard or 5 μl of working solutions of either I3C or DIM in addition to 1 μl of IS (0.4 mg/ml) and used for evaluation of linearity, accuracy and precision of the method.

3.3.4 Extraction Procedure

Aliquots of 50 μl of blank rat plasma, spiked plasma, or pharmacokinetic samples were vortexed for 2 min and allowed to equilibrate 10 min at room temperature. The samples were extracted by adding 200 μl of a premixed solution of diisopropyl ether and ethanol (90:10 v/v respectively) followed by vortex mixing of the samples for 2 min and centrifugation at 10000 rpm for additional 2 min. The organic layer was removed into a clean 2 ml plastic vial. The extraction procedure was repeated one more time and the organic layers were combined. The samples were filtered through 0.22 μm nylon filters and evaporated to dryness under a stream of nitrogen. Samples were reconstituted using 100 μl of 50:50 v/v Acetonitrile: 25 mM Tris Base buffer. On analysis of pharmacokinetic samples, if the I3C or DIM concentration was beyond the upper limit of quantification (20 μg/ml), the samples were diluted to a concentration within the calibration range.

3.3.5 Instrumentation and Chromatographic Conditions

Sample analysis was performed using an Acquity ultra high performance liquid chromatography (UPLC) system (Waters, Milford, MA) equipped with a quaternary solvent delivery unit, a binary pump, a column heater, an autosampler configured with a 10 μl loop and 4^0 C cooler, a built-in degasser, a PDA detector, and a single quadrupole mass detector (SQD) with positive electrospray ionization (ESI) mode. Waters Empower software was used for data acquisition and processing. Chromatographic separations were achieved using an Acquity HSS T3, 1.8 μm 2.1 x 150 mm column (Waters, Milford, MA). The method used an aqueous mobile phase A (MPA) composed of 20 mM of formic acid plus 20 mM of ammonium formate and an organic mobile phase B (MPB) composed of acetonitrile. Furthermore, a weak wash solution (1500 μl)

composed of Milli-Q water and acetonitrile (98:2 v/v), a strong wash solution (500 µl) composed of acetonitrile and water (90:10 v/v respectively), and a seal wash (500 µl) with the same composition as that of the weak wash were used successively between injections to clean and seal the column. The column temperature was set to 35 ± 5 ^{o}C and the autosampler temperature was set to 15 ± 10 ^{o}C. The method was robust using the given column and autosampler temperatures. The injection volume was 10 µl. The gradient was set to 70:30 (MPA:MPB) for the first 7 minutes, 20:80 (MPA:MPB) for one additional minute, and back to initial equilibration status for one additional minute. The run time was 9 min and the flow rate 0.3 ml/min throughout the entire run. The SQD mass detector was operated in the positive electrospray ionization mode (ESI). The following were the final optimized parameters: source temperature, 150 ^{o}C; desolvation temperature, 250 ^{o}C; cone voltage, 41 V; and capillary voltage, 2.66 kV. Peak quantification was achieved using PDA data extracted at 277 nm while peak identification was achieved using the SQD ESI data.

3.3.6 UPLC/MS Method Validation

3.3.6.1 Specificity and Selectivity

Matrix interference was evaluated by comparing chromatograms of blank rat plasma, plasma samples spiked with I3C, DIM and IS, as well as rat pharmacokinetic plasma samples. Additionally, control pharmacokinetic samples obtained after administering the individual delivery vehicles described earlier were evaluated.

3.3.6.2 Sensitivity

The lower limit of quantification (LLOQ) was defined as the lowest concentration yielding a signal to noise ratio of ten. The lowest limit of detection (LLOD) was considered as the concentration resulting in a signal to noise ratio of three.

3.3.6.3 Linearity

Linear regression analysis was used to assess the linearity of the calibration curves for both I3C and DIM. The regression profiles were obtained by plotting the peak area ratios of I3C/IS or DIM/IS against I3C or DIM concentration. Acceptable correlation coefficients (r) for linearity curves were ≥ 0.99.

3.3.6.4 Precision and Accuracy

Intraday (n = 6) and interday (n = 4) accuracy and precision was assessed by analysis of QC samples of I3C or DIM at low (0.25 μg/ml), medium (5.0 μg/ml), and high concentrations (15 μg/ml). The intraday precision and accuracy of the assay was evaluated by calculating the relative standard deviation (RSD) and percent accuracy (average measured concentration/actual concentration * 100) for QC samples on the same day while the interday precision and accuracy was determined over four different days. The acceptance criterion for precision was ≤ 20 % RSD for the LLOQ and ≤ 15 % RSD for higher concentration levels. Similarly, the acceptance criterion for accuracy was a mean value of ≤ 20 % for the LLOQ and ≤ 15 % for higher concentration levels compared to the actual values.

3.3.6.5 Recovery

The extraction recoveries of I3C and DIM were separately determined using extracted QC plasma samples in triplicate and achieved by comparison of the peak area ratios of I3C/IS or DIM/IS with the ratios obtained from standards solutions prepared at equivalent concentrations.

3.3.6.6 Stability

Triplicate QC plasma samples at low (0.5 μg/ml) and high (20.0 μg/ml) concentrations of both I3C and DIM were evaluated for stability at three different conditions: 1) 24 hour thawed at room temperature, 2) three freeze-thaw cycles of 12-24 hours each, and 3) Autosampler stability

after 24 hour first sample post-injection. Long term stability of I3C or DIM in plasma was not evaluated as it has been previously assessed [98] and found to be stable for at least one month at -20 ^{o}C or three months at -80 ^{o}C.

3.3.7 Identification of in vivo I3C Metabolites

The Mass SQD detector was tuned using a mixture of I3C, IS, and DIM. Ion scan optimization was performed as follows: I3C at m/z 130, IS at m/z 148, and DIM at m/z 247. Furthermore, the detector was set to scan ions from 120 to 450 m/z in order to allow identification of additional I3C metabolites.

3.3.8 Application of the validated method to Pharmacokinetic studies of I3C and DIM in rats

The pharmacokinetic parameters were determined by noncompartmental analysis using WinNonlin (version 5.2, Pharsight Corporation, CA). The area under the curve (AUC 0-t) for the concentration-time profiles of both I3C and DIM was calculated from zero to the last time point using the linear/log trapezoidal method and uniform weighting. The maximum plasma concentration (Cmax) and the time to reach maximum plasma concentration (Tmax) after oral administration of DIM (200 mg/kg) were determined by visual inspection of the experimental data. The terminal half life ($t_{½}$) was calculated as 0.693/Kel, where Kel was the slope of the terminal regression line. The bioavailability (F) of DIM after p.o. administration was calculated using the following equation:

F = (oral AUC 0-t * i.v Dose / i.v AUC 0-t * oral Dose) * 100

Total systemic clearance (CL) was calculated as the Dose/AUC 0-∞. The volume of distribution (Vdss) was determined by CL/Kel.

3.4 Results and Discussion

3.4.1 Method Development

In preparing the mobile phase, a combination of ammonium formate and formic acid in water produced excellent buffering conditions that resulted in optimal peak shape and acceptable peak tailing (1.1- 1.5) for I3C, DIM and internal standard. Such aqueous buffer also enhanced the mass detector signal. To maintain stable conditions of I3C, the chosen buffer for sample dilution or reconstitution was a combination of acetonitrile and 25 mM of Tris buffer (50:50 v/v). In order to ascertain stability of each component under these conditions, samples were initially evaluated alone or in the form of a mixture containing I3C, DIM and IS and monitored for potential oligomerization products. All compounds were stable under the described conditions. Several columns were evaluated (data not shown) but HSS T3 (1.8 μm 2.1 x 150 mm) provided the most optimal retention and resolution properties for the mixture. The gradient elution was carefully chosen to allow not only good separation of I3C, DIM and IS but also to allow good separation and identification of other I3C metabolites in the pharmacokinetic studies.

3.4.2 Method Validation

3.4.2.1 Specificity and Selectivity

Retention times for I3C, IS and DIM were approximately 2.5, 4.2, and 5.6 respectively. Figure 3.2 shows representative chromatograms of extracted blank plasma (A), plasma spiked with I3C, IS, and DIM (B) and plasma from the pharmacokinetic studies (C,D,E,F,G). Neither endogenous plasma peaks nor any of the in vivo metabolites of I3C were found to interfere or coelute with any of the compounds evaluated. Furthermore, chromatographic profiles of control pharmacokinetic samples after administering the delivery vehicles were equal to those of blank plasma.

3.4.2.2 Sensitivity

Using 50 μl of plasma for extraction, 100 μl for sample reconstitution, and 10 μl as the UPLC injection volume, the LLOD for both I3C and DIM was found to be 15 ng/ml and the LLOQ was 25 ng/ml for both I3C and DIM. The latter is two times more sensitive than previously reported [98].

3.4.2.3 Linearity

Plasma calibration curves for both I3C and DIM were linear over the concentration range of 0.025-20 μg/ml. The intra and inter-day calibration curves showed consistent linearity as determined from the intercept, slope, and coefficients of correlation. The mean regression equation ± SD of triplicate calibration curves obtained on separate days were $y = (0.01262 \pm 0.004)x - (0.0027 \pm 0.002)$ for I3C and $y = (0.1268 \pm 0.002)x - (0.023 \pm 0.01)$ for DIM. Correlation coefficients were 0.9996 ± 0.002 for I3C and 0.9947 ± 0.004 for DIM.

3.4.2.4 Precision and Accuracy

Precision and accuracy of the method were evaluated according to the CDER Guidance for Industry in Bioanalytical Method Validation [78]. Low (0.25 μg/ml), medium (5.0 μg/ml), and high (15.0 μg/ml) QC plasma samples of both I3C and DIM were used to assess the precision (RSD) and accuracy of the method. Intraday precision ranged from 1.67 to 2.18% for I3C and from 1.28 to 2.35% in the case of DIM. Similarly, I3C interday precision ranged from 1.66 to 12.90% and that of DIM ranged from 0.58 to 11.66%. Additionally, respective intraday and interday accuracy ranged from 96.94 to 112.43 % and 97.10 to 103.44 % for I3C while they ranged from 96.83 to 114.11% and 98.98 to 112.14 % for DIM. Table 3.1 provides a detailed summary of the values, which clearly show that the precision and accuracy values were well within the acceptance range.

3.4.2.5 Recovery

A comparison of the ratios of I3C/IS or DIM/IS obtained from the extracted QC plasma samples to the ratios of sample solutions prepared at equivalent concentrations resulted in excellent mean recovery of 96.21 ± 0.23% for I3C and 108.5 ± 0.96% for DIM.

3.4.2.6 Stability

Stability of stock solutions as well as long term stability of spiked I3C or DIM plasma samples have previously been demonstrated [98] and therefore were not assessed in this study. Only short term, freeze thaw, and autosampler stability were evaluated and successfully demonstrated. Stability studies were carried out according to the CDER guidelines [78]. Triplicate samples of concentrations of I3C or DIM in plasma at low (0.5 μg/ml) and high (20 μg/ml) concentration levels were used. Stability of I3C or DIM in plasma samples was assessed by comparing the I3C/IS or DIM/IS ratios to those of freshly prepared and processed samples and was expressed as percent remaining. The samples were stable at all conditions tested and the results are summarized in Table 3.2. I3C or DIM plasma samples were stable after 24 hour thaw periods at room temperature. Spiked plasma samples were also stable after three freeze-thaw cycles for time intervals between 12 to 24 hours. Lastly, stability of the samples in reconstitution buffer was demonstrated after 24 hours in the autosampler.

3.4.3 Identification of in vivo I3C Metabolites

At least six in vivo I3C metabolites: indole-3-carboxaldehyde (I3A; RT: 4.5; m/z 130), di-1H-indol-3-ylmethanol (DIMOH; RT: 5.1; m/z 259), 3,3-diindolylmethane (DIM; RT: 5.6; m/z 247), di-1 H-indol-3-ylmethanone (DIMO; RT: 6.7; m/z 249), [1-(3-hydroxymethyl)-indolyl-3-indolylmethane (HI-IM; RT: 6.4; m/z 275), and indole-[3,2*b*]-carbazole-6,12-(5*H*,11*H*)-dione (ICZO; RT: 6.9; m/z 287) were identified after i.v. or i.p. administration (Fig 3.2C,D,E). I3C

metabolites were the same after i.v. (25 mg/kg) or i.p. (100 mg/kg) administration of I3C given as a suspension in the polymeric delivery vehicle described earlier. Interestingly, i.p. administration of I3C (50 mg/kg) suspended in olive oil and DMSO resulted in only three metabolites: indole-3-carboxylic acid (I3CA; RT: 2.9; m/z 130), DIMOH, and DIM (Figure 3.2C), two of which were also found after administration of I3C in the polymer vehicle and one which was specific to the DMSO:Olive oil suspension. Some of the metabolites (i.e. I3A, I3CA, DIM, and HI-IM) identified in this article agree with previous findings [95, 98], while other metabolites (DIMOH, DIMO, and ICZO) were newly identified metabolites. Very interestingly, however, none of the metabolites was of trimeric nature (i.e. Ltr1, CT) as previously reported [95, 98]. It is possible that formation of trimeric or higher molecular weigh I3C metabolites may be favored only under very acidic conditions as those provided by the stomach. Since administration of I3C was via i.v. or i.p. routes and because the systemic pH in the intraperitoneal or central systemic compartments is higher than that in the stomach, the formation of such high MW metabolites was not seen. The absence of trimeric products in this study was in agreement with previous studies by Reed et al. [50] where trimeric products were not detectable even after administration of high oral doses above 400 mg to women. Based on the ion masses (Figure 3.2H) and retention times obtained for such metabolites, structures have been proposed (Figure 3.1). However, true elucidation of the proposed metabolites may only be achieved using MS/MS techniques. On the other hand, DIM (Figure 3.2F,G) was very stable and did not form any metabolites *in vivo*.

3.4.4 Application of the validated method to Pharmacokinetic studies of I3C and DIM in rats

The validated UPLC/MS method was successfully applied to the evaluation of pharmacokinetic (PK) profiles and parameters in Sprague Dawley rats. Figure 3.3 shows the PK profiles of (A) I3C following i.v. (25 mg/kg) or i.p. (50 mg/kg and 100 mg/kg) administration and (B) DIM after i.v. (20 mg/kg) or single p.o. dose (200 mg/kg) administration. The PK parameters (Table 3.3) for the plasma concentration-time profiles were obtained by noncompartmental analysis using WinNonlin. Additionally, the PK profiles for I3C metabolites upon administration of I3C via i.v. or i.p. routes are shown in Figure 3.4(A,B,C) and were approximated using I3C or DIM calibration curves depending on the nature of the metabolite. Nonetheless, true concentrations may vary from the values reported here as their relative response factors were unknown, except for DIM.

Evidently, metabolic bio-transformation of I3C was very rapid as seen in Figure 3.4 (A,B,C) and the concentration of most metabolites was clearly higher than that of I3C at all time points including initial timepoints. Such findings were in line with previous observations [50] in which DIM was the only quantifiable product upon the oral administration of I3C to women but contrary to [48] where I3C was the predominant product after an oral dose of 250 mg/ml to mice. Noncompartmental PK parameters were estimated for the major metabolites (DIM and HI-IM) of I3C (Table 3.4). The concentration-time profiles after i.v. or i.p. administration of I3C as well as after i.v. administration of DIM clearly exhibited multi-exponential concentration decline with rapid distribution and absorption phases and slow first order elimination. On the other hand, the oral PK profile of DIM exhibited slow absorption phase and slow mono-exponential first order decay.

The AUC of DIM after an i.v dose of 20 mg/kg was 19-fold higher than the AUC of I3C after i.v. administration of 25 mg/kg. This is most likely due to the high stability of DIM and relative

quick metabolism of I3C. Additionally, the DIM systemic exposure after administering DIM (20 mg/kg i.v.) as the parent drug or after administering I3C (25 mg/kg i.v.) as the pro-drug for DIM was comparable (11.9 ± 5.9 μg*h/ml versus 19.7 ± 5.8 μg*h/ml respectively), which one more time confirms high i.v. metabolism of I3C.

DIM was poorly bioavailable (7.0 ± 8.4%) after oral administration given as a polymer suspension. This may be attributed to low gastrointestinal absorption which again may partly be due to the limited solubility of DIM in the polymeric delivery vehicle which rather formed a homogeneous nanoparticle-like suspension. Gastrointestinal first pass metabolism may be ruled out since no metabolites were observed after DIM oral dosing. The latter observation was in agreement with previous studies in mice [49]. Contrary to studies in [49] where the mean plasma AUC after administration of 250 mg/kg to mice was 25.4 μg*h/ml, the mean oral DIM AUC obtained for the formulation used in this study was 5.1 ± 2.7 μg*h/ml, which is ~ 4 times less in systemic exposure. This difference is most likely due to the use of an absorption enhanced DIM formulation by Anderton et al. [49] even though species differences should not be discarded. This is however, to the best of our knowledge, the first studies to show absolute bioavailability of DIM in rats based on i.v. and p.o. dosing regimens. It is noteworthy to mention that despite the low oral bioavailability of DIM, the apparent terminal half life was about12 ± 4.3 hours clearly due to small changes in plasma concentration between 8 and 18 hours. This value is higher than reported (~ 4 hours) in [49, 51] for the absorption enhanced DIM formulation. Indeed, the concentration versus time data resembled a slow-release PK profile.

In this study, after i.p administration of 50 mg/kg of I3C in the olive oil/ DMSO formulation, the AUC (23.9 ± 4.4 μg*h/ml) was significantly higher ($p < 0.05$) than the AUC of both i.p.

administration of 100 mg/kg (0.71 ± 0.06 μg*h/ml) in the polymeric vehicle and i.v. administration of 25 mg/kg of I3C (0.62 ± 0.14 μg*h/ml) in the same polymer vehicle. Such increased AUC is evidently due to the observed low CL (2.15 ± 0.42 L/h/kg) and Vdss (0.64 ± 0.52 L/kg) in the peritoneal cavity as a result of the DMSO/olive oil formulation; therefore suggesting a marked advantage for regional i.p. delivery of I3C using such drug delivery vehicle. However, the mean $t_{1/2}$ for this dosing regimen was less than an hour and would most likely require an infusion therapy which is not normally desired. On the other hand, the low AUC observed with the 100 mg/kg i.p. dose of I3C can be explained by the rapid I3C clearance (120 ± 16 L/h/kg) from the peritoneal cavity. The fast clearance may be due to the rapid biotransformation of I3C into major metabolites such as DIM or HI-IM for which the estimated AUC exposure levels (72.3 ± 15.36 and 61.4 ± 13.95 μg*h/ml respectively) were more than 100-fold higher compared to parent I3C.

Additionally, compartmental models were fitted for the plasma concentration-time profiles of I3C 50 mg/kg i.p (Figure 3.5), I3C 100 mg/kg i.p (Figure 3.6), I3C 25 mg/kg i.v. (Figure 3.7), DIM 200 mg/kg (Figure 3.8), and DIM 20 mg/kg (Figure 3.9). Compartmental PK parameters are presented in Table 3.5. The concentration-time profiles of I3C after i.v, or i.p administration or DIM after i.v administration were well fitted by two-compartment models whereas the PK profile following p.o administration of DIM was well fitted by a one-compartment model. Goodness of model fit was shown by the low Akaike information criterion (AIC), Cross-validation (CV) and total weighted sum of square residuals (TWSSR) (Table 3.5).

3.5 Conclusion

A rapid, sensitive, and reliable UPLC/MS method with excellent recovery, selectivity, precision, and accuracy has been developed and validated for the first time for analysis of I3C and its metabolites including DIM. The method has been successfully applied to the assessment of pharmacokinetic profiles and parameters after i.v. or i.p. administration of I3C as well as i.v. and p.o administration of DIM to rats. At least three metabolites not previously reported before were proposed in the current studies. Furthermore, with a short run time, the method will allow high throughput analysis of pharmacokinetic samples and will ease development and validation of other UPLC methods for analysis of I3C and related compounds in other biological matrixes. Very importantly, we also have demonstrated that UPLC/MS provides an excellent opportunity for the elucidation of new metabolites unable to be resolved by conventional HPLC. This benefit, in turn, will generate new inroads into the understanding of the true metabolic fate of compounds.

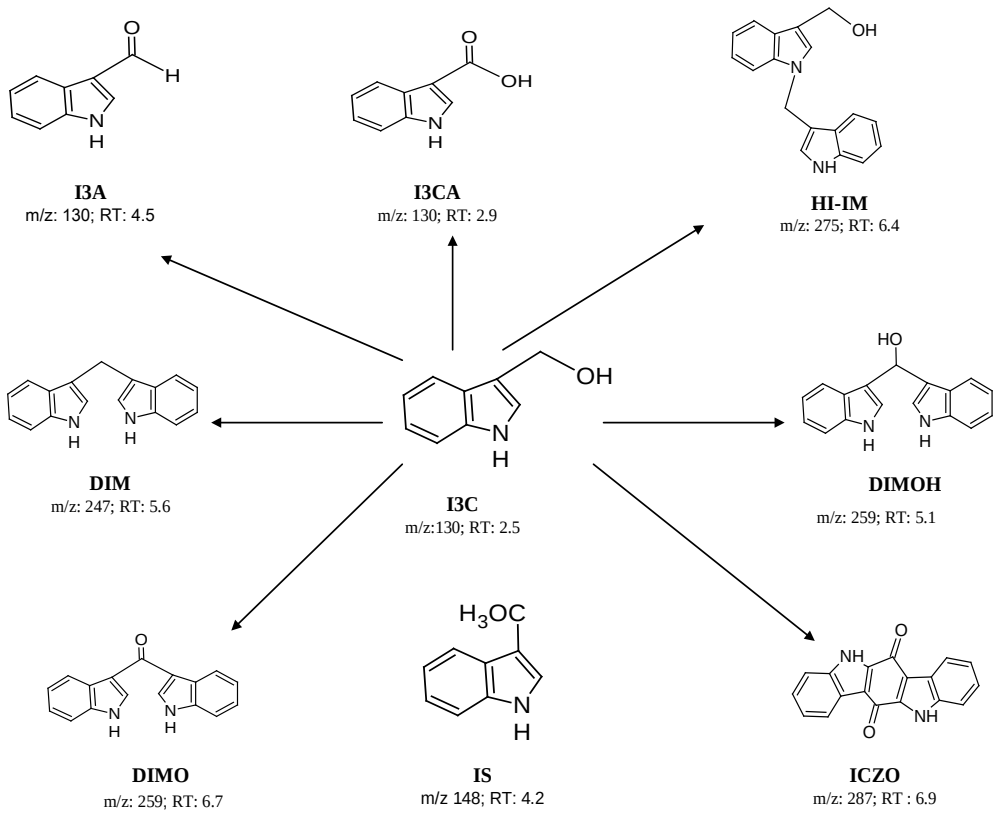

Fig. 3.1. Chemical structures[7] of I3C, DIM, and IS and proposed structures of I3C metabolites. RT: retention time; m/z: ionization mass obtained by mass spectrometry analysis in positive ESI mode. Structures of I3A, I3CA, and HI-IM were in agreement with [48] and DIM was in agreement with previous findings [48, 98]. Proposed structures of DIMO, DIMOH and ICZO were newly encountered metabolites.

[7]**Abbreviation**s:I3C, indole-3-carbinol; DIM, 3,3-diindolylmethane; IS, internal standard (4-Methoxy Indole); ESI, electron spray ionization; I3A, indole-2-aldehyde; I3CA, indole-3-carboxylic acid; HI-IM, [1-(3-hydroxymethyl)]-indolyl-3-indolylmethane; DIMO, di-1-*H*-indol-3-ylmethanone; DIMOH, di-1-*H*-indol-3-ylmethanol; ICZO, indole-[3,2*b*]carbazole-6,12-(5*H*, 11*H*)-dione.

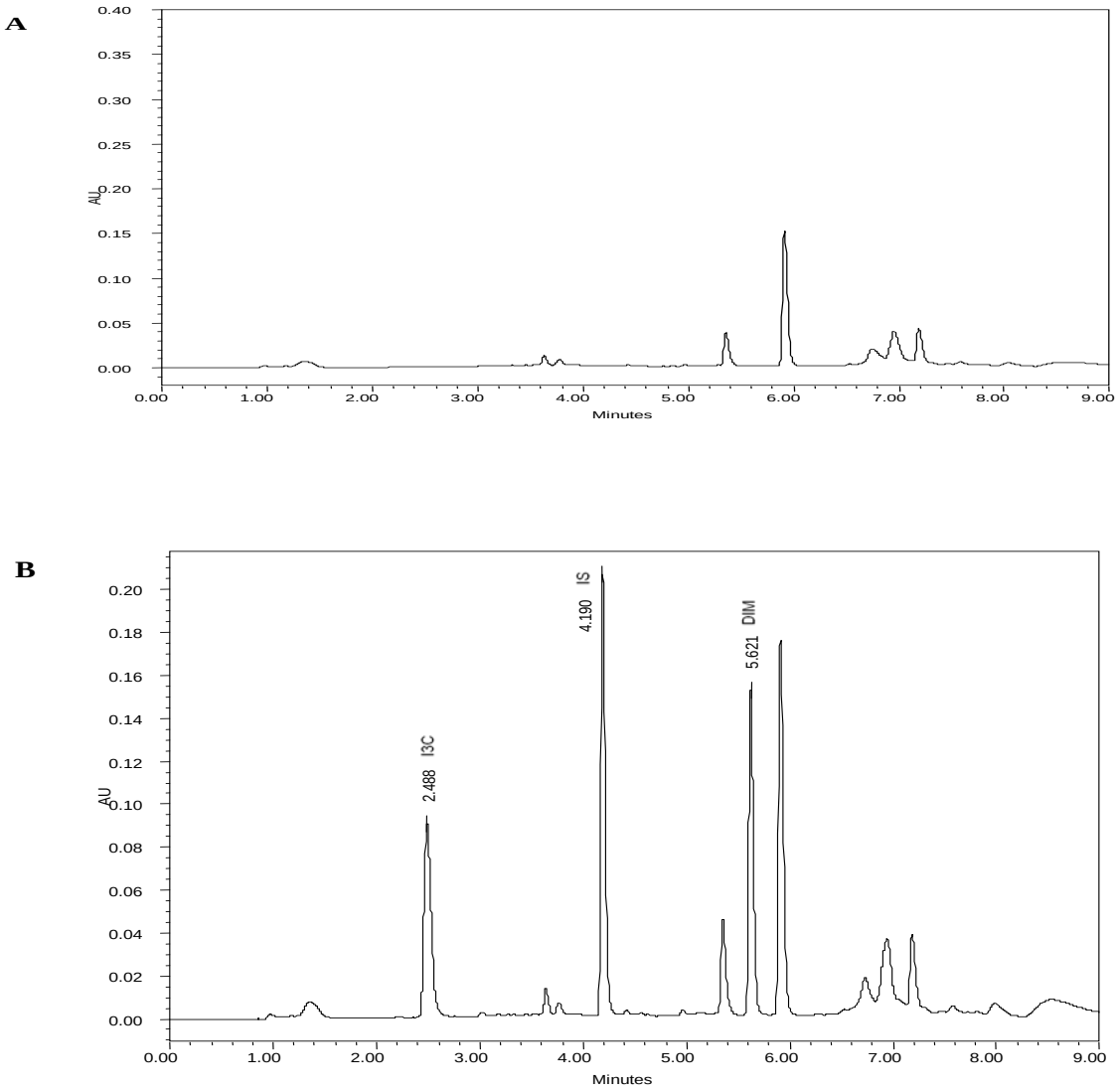

Fig.3.2. (Cont'd) Representative chromatograms of (A) blank rat plasma; (B) blank rat plasma spiked with I3C, DIM, and IS[8]**.**

[8]**Abbreviation**s:I3C, indole-3-carbinol; DIM, 3,3-diindolylmethane; IS, internal standard (4-Methoxy Indole).

C

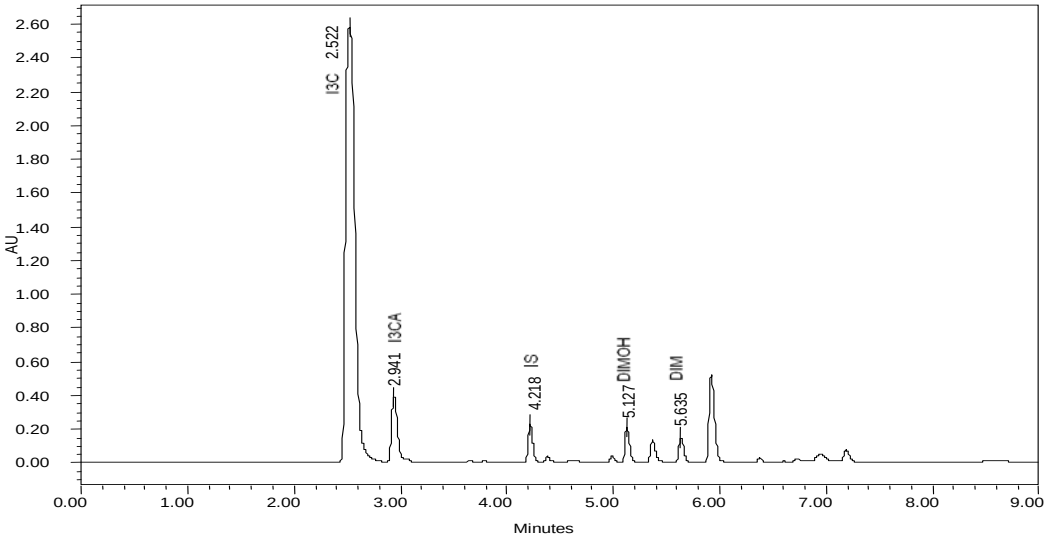

Fig.3.2. (Cont'd) Representative chromatogram of (C) rat plasma sample at 2 min after i.p. administration of I3C (50 mg/kg)[9].

[9]**Abbreviation**s:I3C, indole-3-carbinol; DIM, 3,3-diindolylmethane; IS, internal standard (4-Methoxy Indole); I3CA, indole-3-carboxylic acid; DIMOH, di-1-*H*-indol-3-ylmethanol.

D

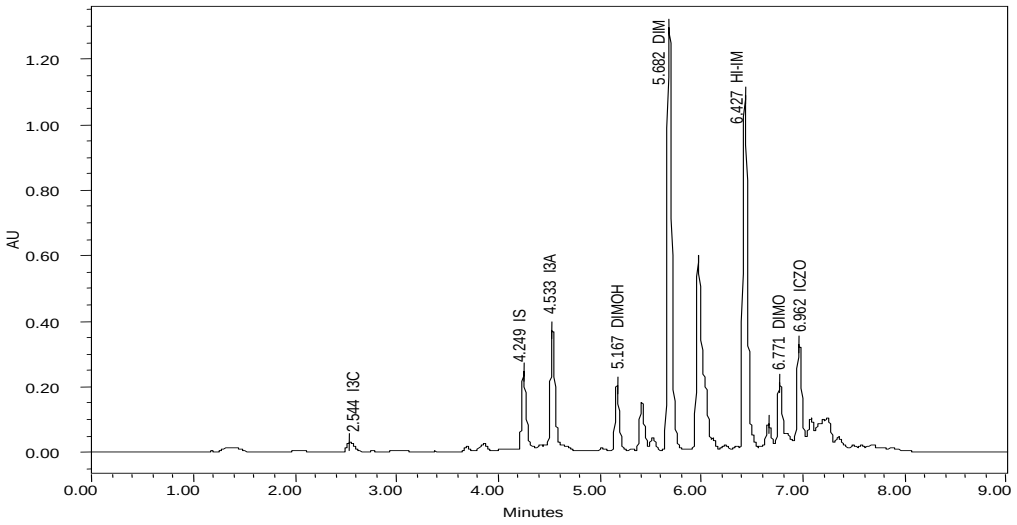

Fig.3.2. (Cont'd) Representative chromatogram of (D) rat plasma sample at 5 min after i.v. administration of I3C (25 mg/kg)[10].

[10]**Abbreviation**s:I3C, indole-3-carbinol; DIM, 3,3-diindolylmethane; IS, internal standard (4-Methoxy Indole); I3A, indole-2-aldehyde; HI-IM, [1-(3-hydroxymethyl)]-indolyl-3-indolylmethane; DIMO, di-1-*H*-indol-3-ylmethanone; DIMOH, di-1-*H*-indol-3-ylmethanol; ICZO, indole-[3,2*b*]carbazole-6,12-(5*H*, 11*H*)-dione.

E

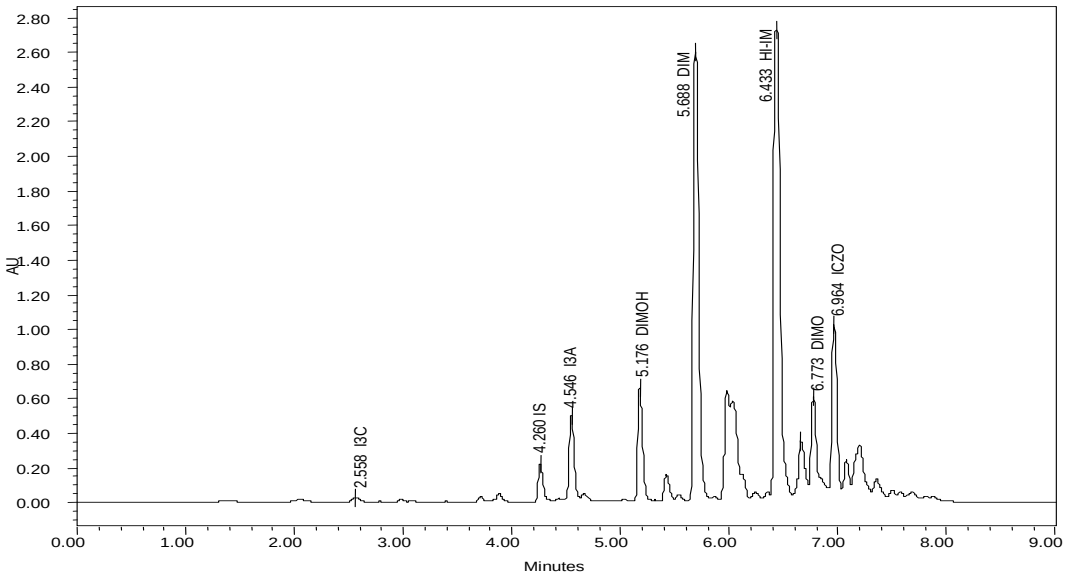

Fig.3.2. (Cont'd) Representative chromatogram of (E) rat plasma sample at 5 min after i.p. administration of I3C (100 mg/kg)[11].

[11]**Abbreviation**s:I3C, indole-3-carbinol; DIM, 3,3-diindolylmethane; IS, internal standard (4-Methoxy Indole); I3A, indole-2-aldehyde; HI-IM, [1-(3-hydroxymethyl)]-indolyl-3-indolylmethane; DIMO, di-1-*H*-indol-3-ylmethanone; DIMOH, di-1-*H*-indol-3-ylmethanol; ICZO, indole-[3,2*b*]carbazole-6,12-(5*H*, 11*H*)-dione.

F

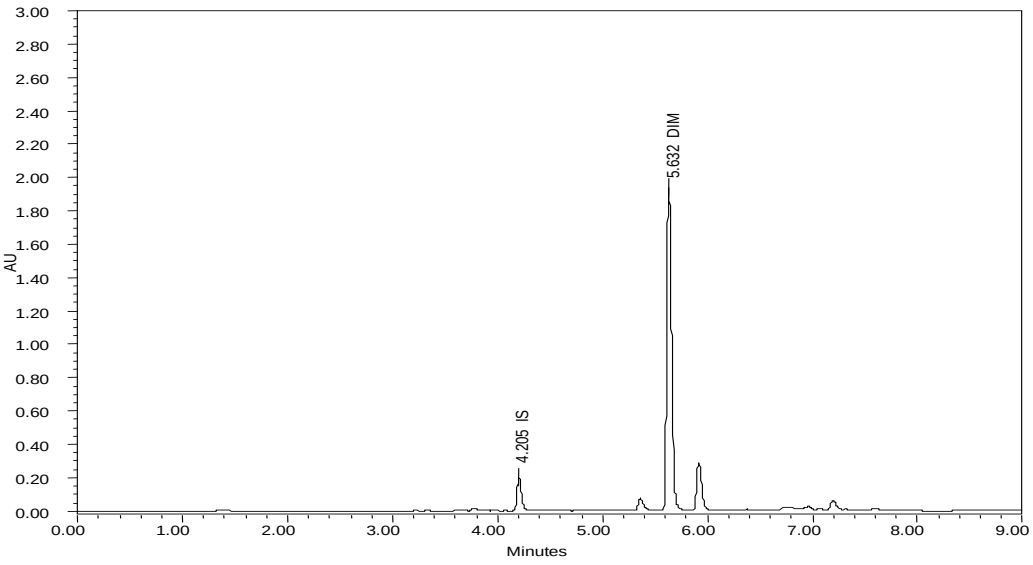

Fig.3.2. (Cont'd) Representative chromatogram of (F) rat plasma sample at 2 min after i.v. administration of DIM (20 mg/kg)[12].

[12]**Abbreviation**s: IS, internal standard (4-Methoxy Indole); DIM, 3,3-diindolylmethane.

G

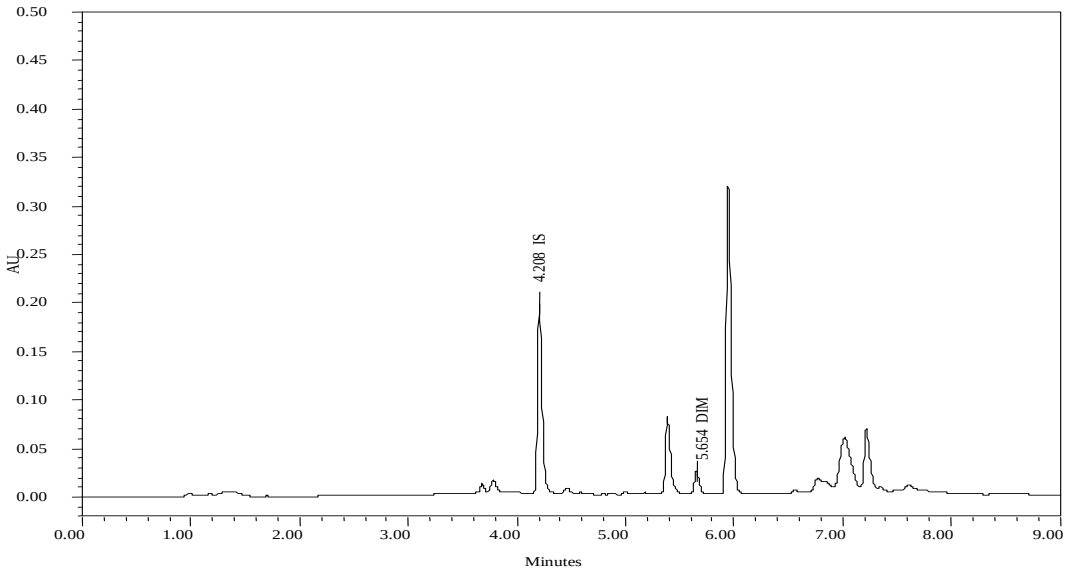

Fig.3.2. (Cont'd) Representative chromatogram of (G) rat plasma sample at 4 hours after p.o. administration of DIM (200 mg/kg)[13].

[13]**Abbreviation**s: IS, internal standard (4-Methoxy Indole); DIM, 3,3-diindolylmethane.

H

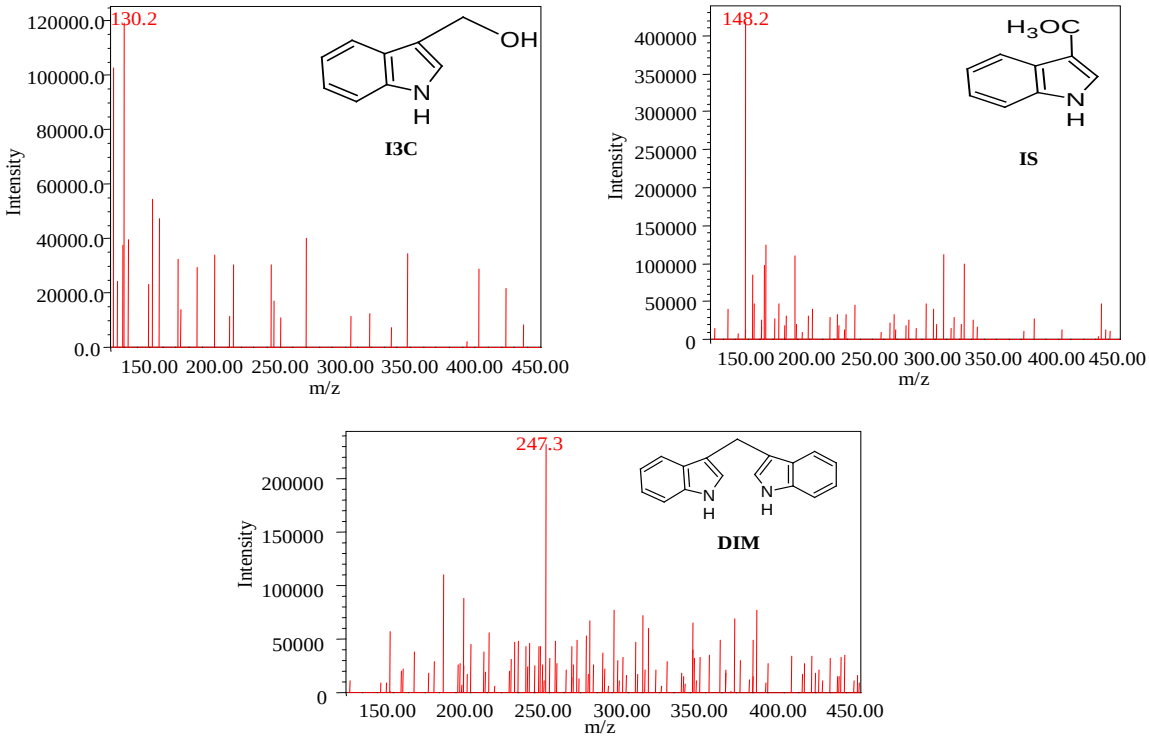

Fig.3.2. (Cont'd) Representative mass spectrograms of (H) I3C, IS, and DIM[14].

[14]**Abbreviation**s:I3C, indole-3-carbinol; DIM, 3,3-diindolylmethane; IS, internal standard (4-Methoxy Indole).

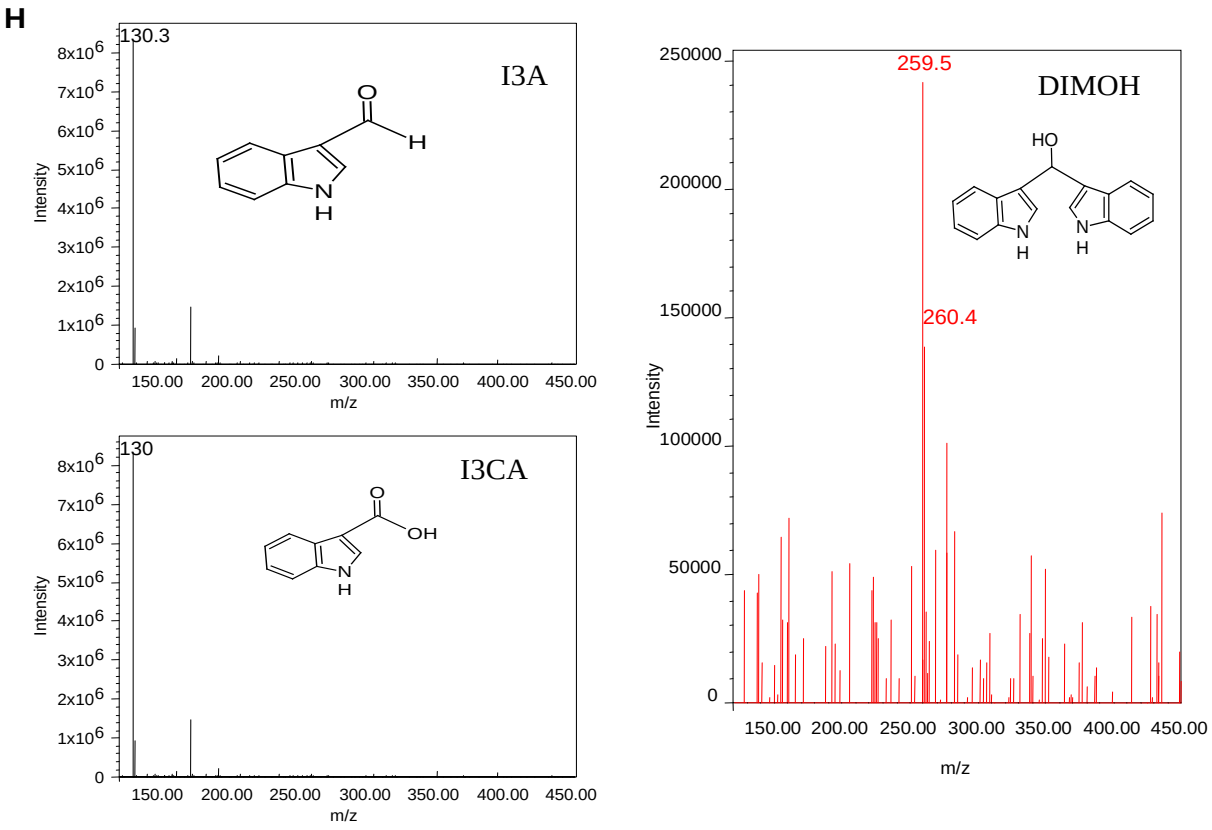

Fig.3.2. (Cont'd) Representative mass spectrograms of (H) I3A, I3CA, and DIMOH[15].

[15]**Abbreviation**s: I3A, indole-2-aldehyde; I3CA, indole-3-carboxylic acid; DIMOH, di-1-*H*-indol-3-ylmethanol.

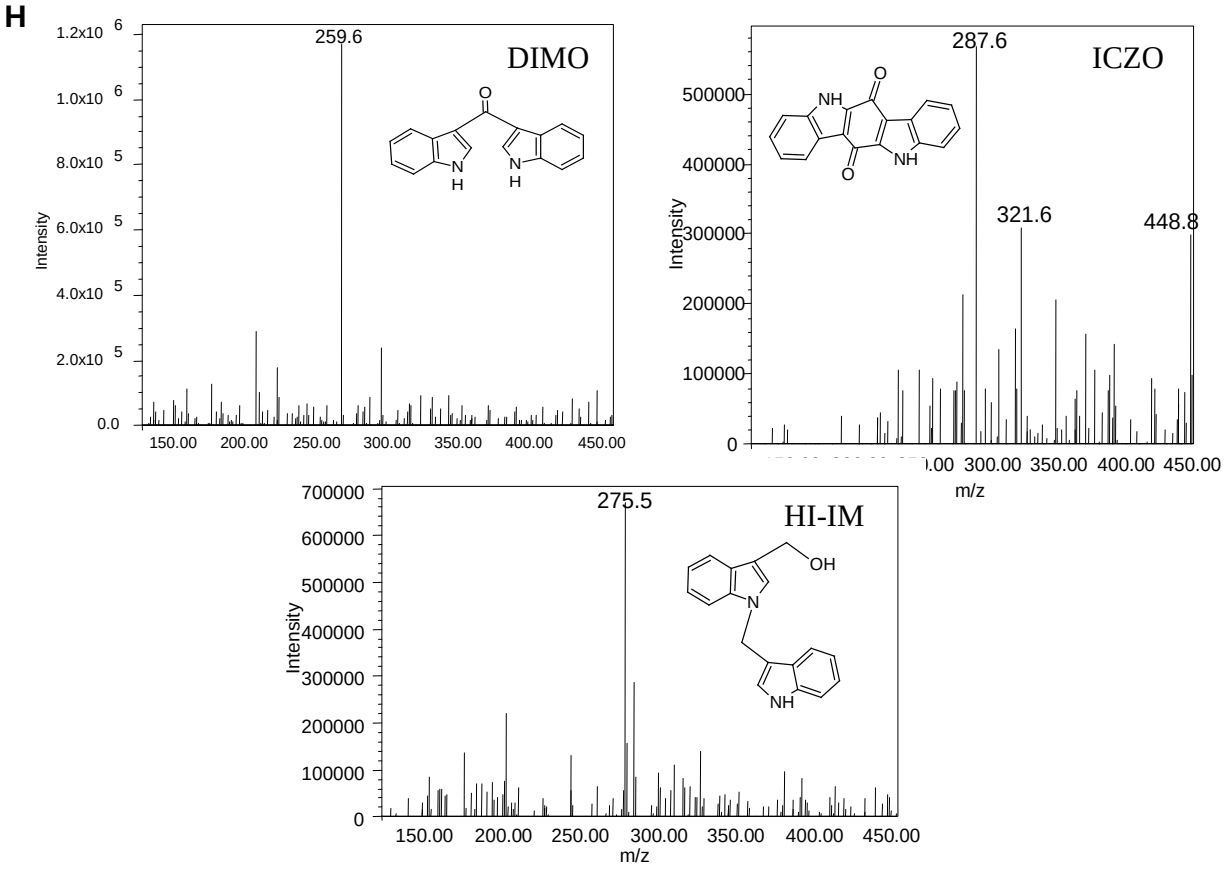

Fig.3.2. (Cont'd) Representative mass spectrograms of (H) DIMO, HI-IM, and ICZO[16].

[16]**Abbreviation**s: DIMO, di-1-*H*-indol-3-ylmethanone; HI-IM, [1-(3-hydroxymethyl)]-indolyl-3-indolylmethane; ICZO, indole-[3,2*b*]carbazole-6,12-(5*H*, 11*H*)-dione.

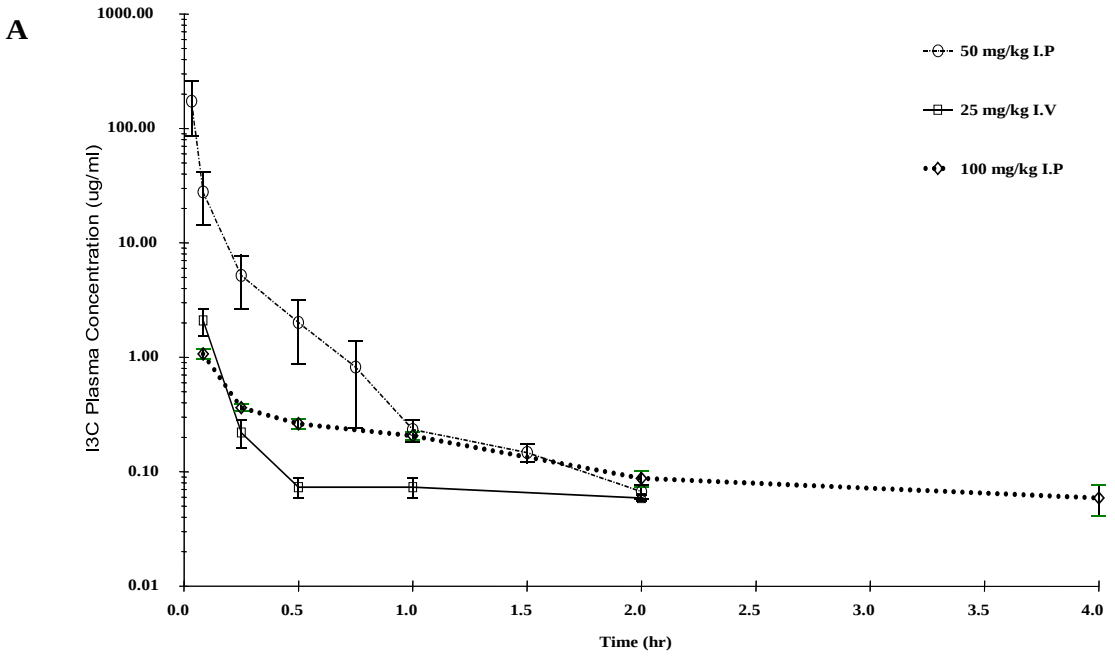

Fig.3.3 Mean pharmacokinetic profiles of (A) I3C administration (50 mg/kg and 100 mg/kg i.p. and 25 mg/kg i.v.)[17]; bars represent ± SD of 4-6 animals.

[17]**Abbreviation**s: I3C, indole-3-carbinol

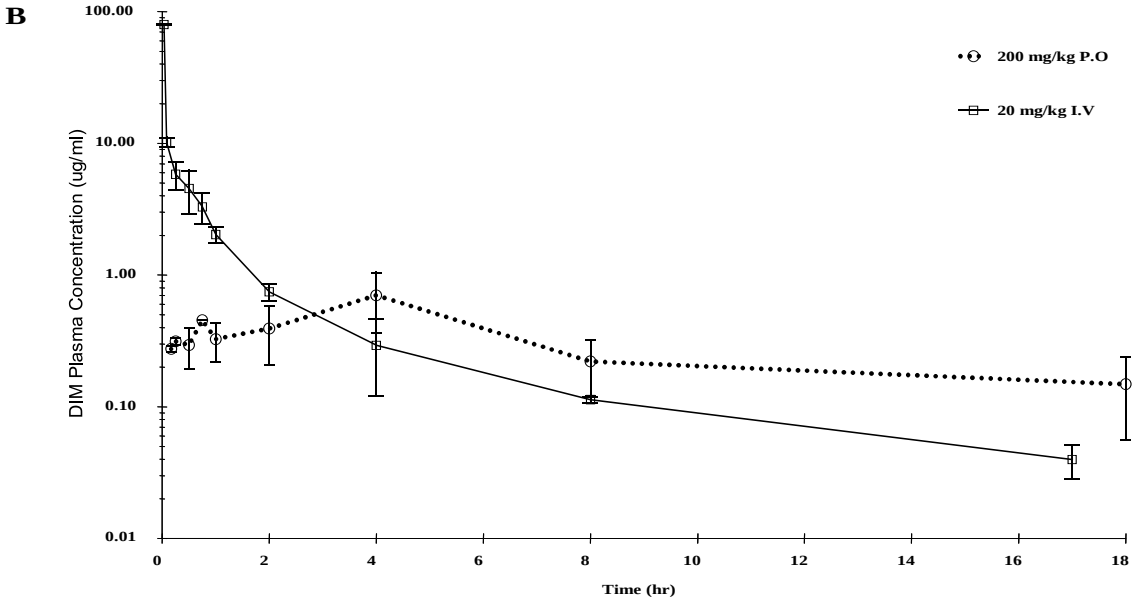

Fig.3.3 (Cont'd) Mean pharmacokinetic profiles of (B) DIM administration (20 mg/kg i.v. and 200 mg/kg p.o.) to Sprague Dawley rats[18]; bars represent ± SD of 4-6 animals.

[18]**Abbreviation**s: DIM, 3,3-diindolylmethane.

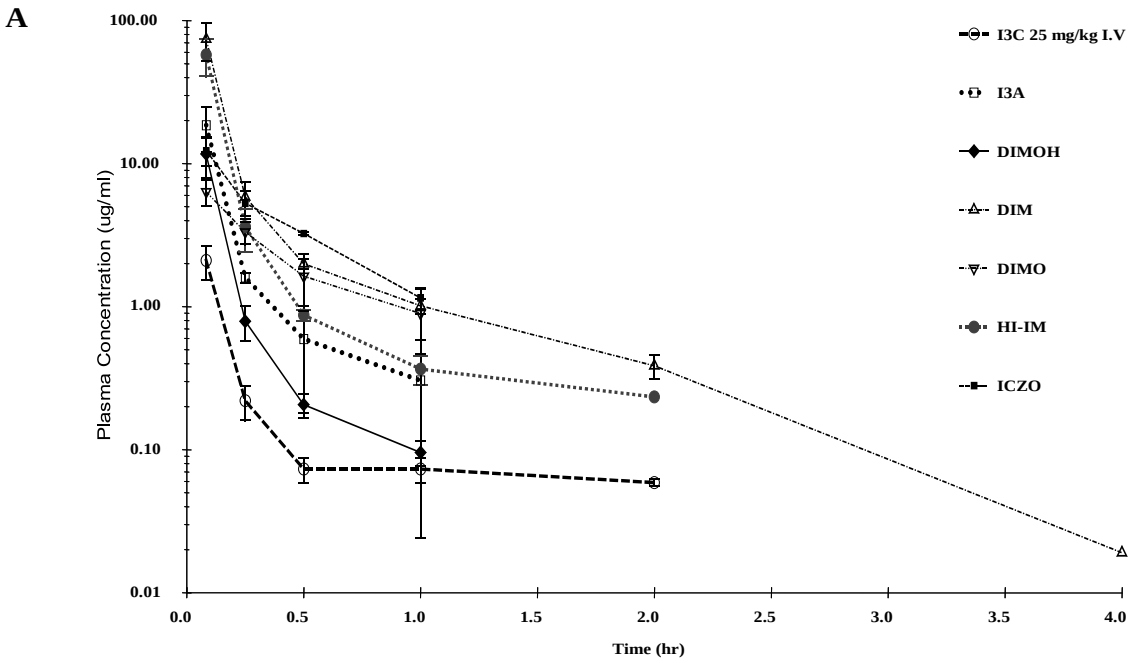

Fig.3.4 Mean pharmacokinetics profiles of I3C metabolites following I3C administration of (A) 25 mg/kg i.v.[19]; bars represent ± SD of 4-6 animals.

[19]**Abbreviation**s:I3C, indole-3-carbinol; I3A, indole-2-aldehyde; DIMOH, di-1-*H*-indol-3-ylmethanol; DIM, 3,3-diindolylmethane; DIMO, di-1-*H*-indol-3-ylmethanone; HI-IM, [1-(3-hydroxymethyl)]-indolyl-3-indolylmethane; ICZO, indole-[3,2*b*]carbazole-6,12-(5*H*, 11*H*)-dione.

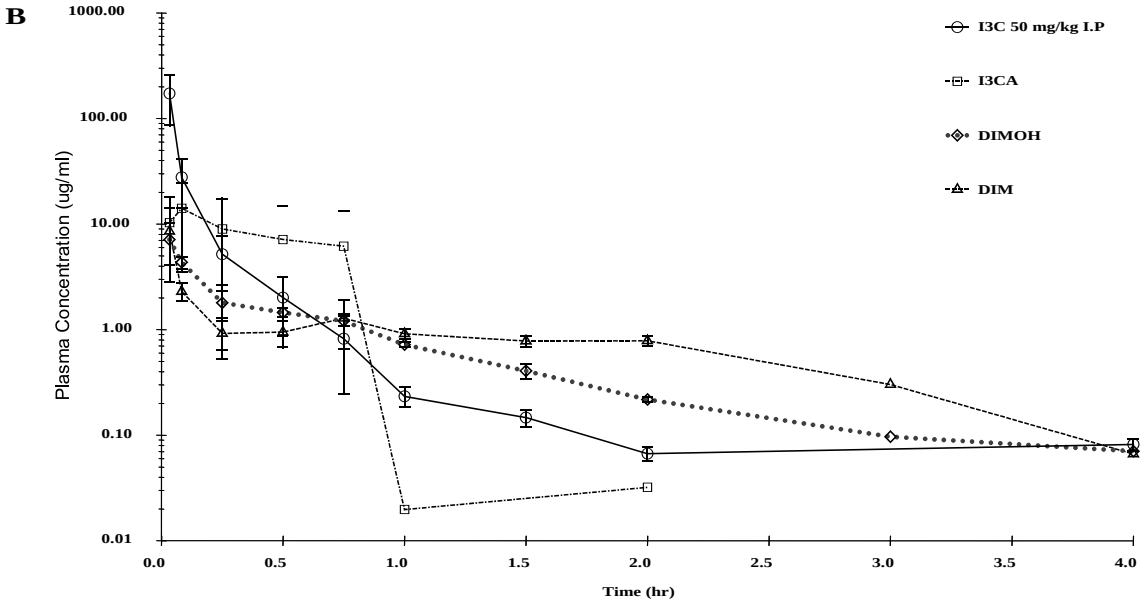

Fig.3.4 (Cont'd) Mean pharmacokinetics profiles of I3C metabolites following I3C administration of (B) 50 mg/kg i.p.[20]; bars represent ± SD of 4-6 animals.

[20]**Abbreviation**s:I3C, indole-3-carbinol; I3CA, indole-3-carboxilic acid; DIMOH, di-1-*H*-indol-3-ylmethanol; DIM, 3,3-diindolylmethane.

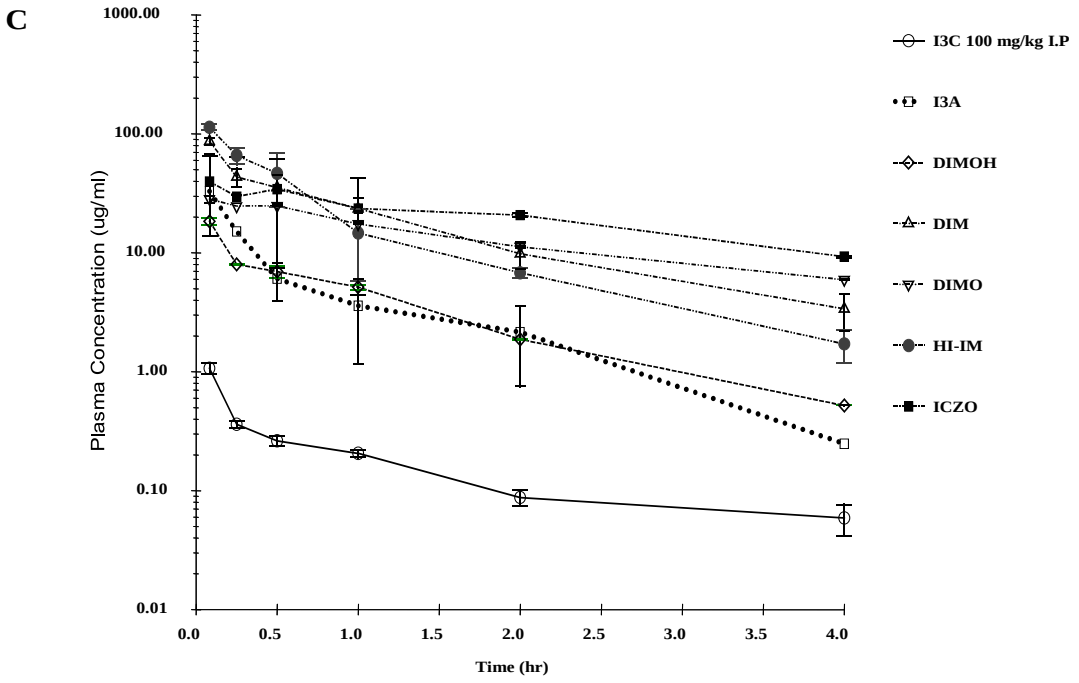

Fig.3.4 (Cont'd) Mean pharmacokinetics profiles of I3C metabolites following I3C administration of (C) 100 mg/kg i.p.[21]; bars represent ± SD of 4-6 animals.

[21]**Abbreviation**s:I3C, indole-3-carbinol; I3A, indole-2-aldehyde; DIMOH, di-1-*H*-indol-3-ylmethanol; DIM, 3,3-diindolylmethane; DIMO, di-1-*H*-indol-3-ylmethanone; HI-IM, [1-(3-hydroxymethyl)]-indolyl-3-indolylmethane; ICZO, indole-[3,2*b*]carbazole-6,12-(5*H*, 11*H*)-dione.

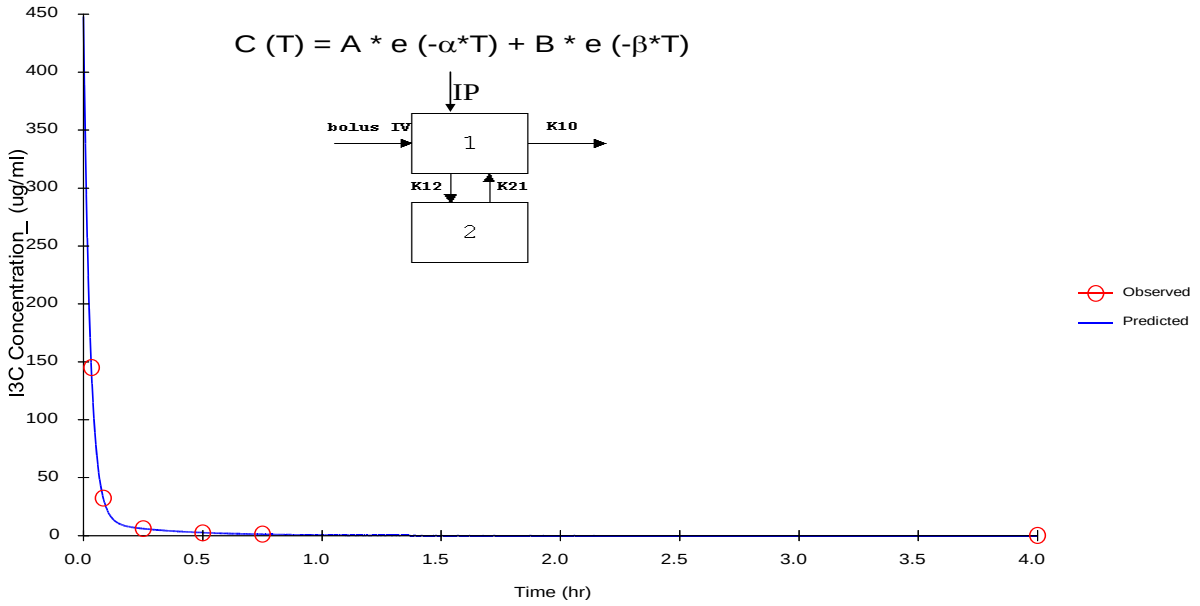

Fig. 3.5 Pharmacokinetic data fitting after i.p. administration of 50 mg/kg of I3C. The pharmacokinetic data was well fitted by a two compartment model as clearly observed from the observed versus predicted data. **Assumptions**: 2 compartment IV-Bolus, micro-constants, no lag time, 1st order elimination. I3C was rapidly absorbed and distributed and it exhibited a slow terminal elimination phase.

$$C(T) = A * e^{(-\alpha * T)} + B * e^{(-\beta * T)}$$

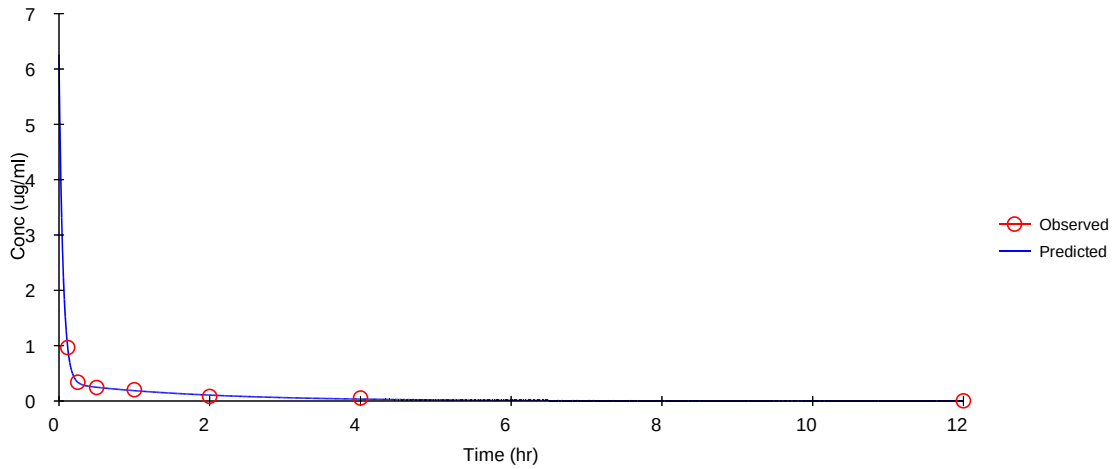

Fig. 3.6 Pharmacokinetic data fitting after i.p. administration of 100 mg/kg of I3C. The pharmacokinetic data was well fitted by a two compartment model as clearly observed from the observed versus predicted data. **Assumptions**: 2 compartment IV-Bolus, micro-constants, no lag time, 1st order elimination. I3C was rapidly absorbed and distributed and it exhibited a slow terminal elimination phase.

$$C(T) = A * e^{(-\alpha * T)} + B * e^{(-\beta * T)}$$

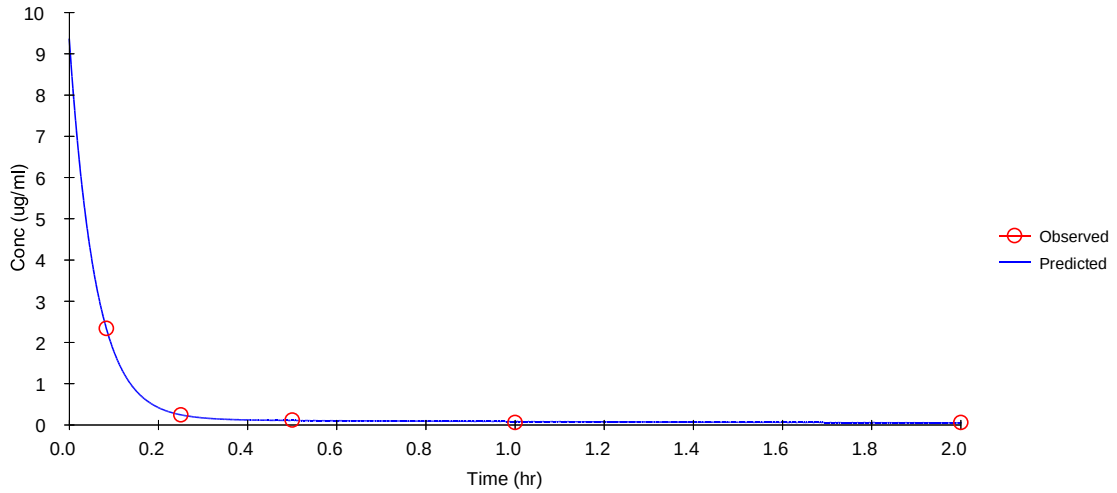

Fig. 3.7 Pharmacokinetic data fitting after i.v. administration of 25 mg/kg of I3C. The pharmacokinetic data was well fitted by a two compartment model as clearly observed from the observed versus predicted data. **Assumptions**: 2 compartment IV-Bolus, micro-constants, no lag time, 1st order elimination. I3C was rapidly absorbed and distributed and it exhibited a slow terminal elimination phase. The I3C concentration in the central compartment reached ~50 % of its maximum concentration in plasma in about 15 minutes, suggesting a very quick clearance mechanism.

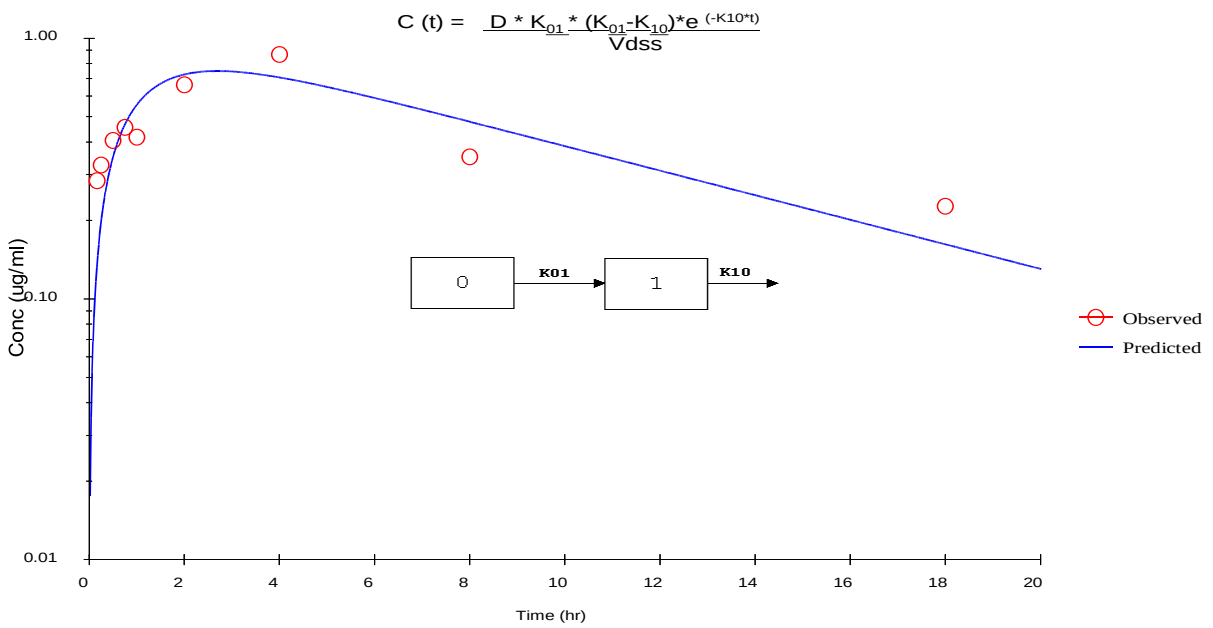

Fig. 3.8 Pharmacokinetic data fitting after p.o. administration of 200 mg/kg of DIM. The pharmacokinetic data was well fitted by a one compartment model as clearly observed from the observed versus predicted data. **Assumptions**: 1 compartment, micro-constants, lag time, first order elimination. DIM was slowly absorbed and exhibited a lag time of at least 15 minutes. The apparent terminal elimination phase was very slow suggesting that the DIM formulation resembled a slow release profile with possible sustained release properties.

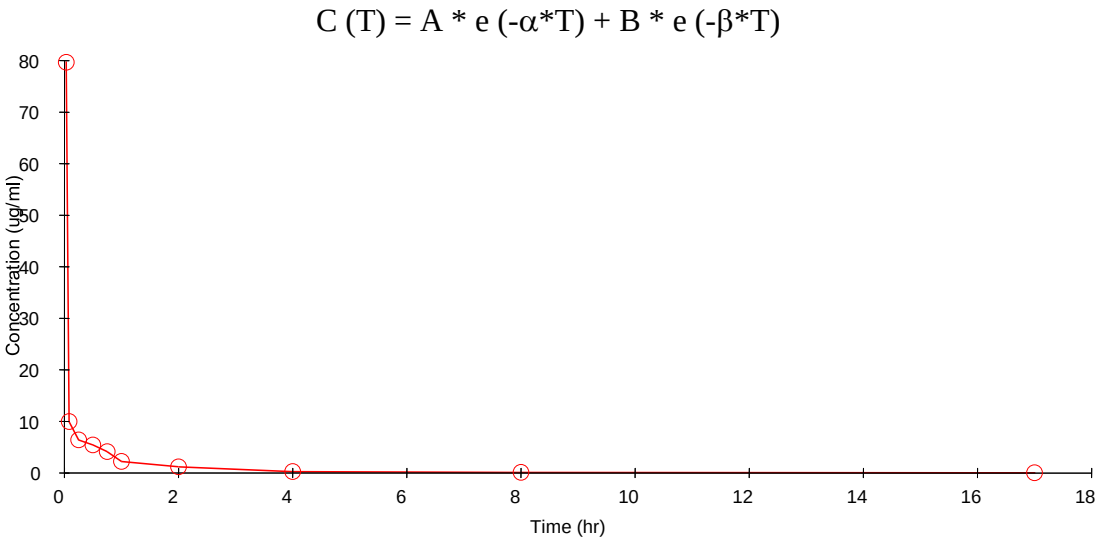

Fig. 3.9 Pharmacokinetic data fitting after i.v. administration of 20 mg/kg of DIM. The pharmacokinetic data was well fitted by a two compartment model as clearly observed from the observed versus predicted data. **Assumptions**: 2 compartment IV-Bolus, micro-constants, no lag time, 1st order elimination. DIM was rapidly absorbed and distributed and it exhibited a slow terminal elimination phase. The DIM concentration in the central compartment reached ~50 % of its maximum concentration in plasma in less than 15 minutes, suggesting a very quick clearance mechanism.

Table 3.1

Precision and Accuracy of the method for the quantification of I3C and DIM in Rat Plasma

Concentration (μg/ml)	**Mean (μg/ml)**	**Precision (% RSD)**	**Accuracy (%)**
I3C Intraday (n = 6)			
0.25	0.28 ± 0.01	2.18	112.43
5.0	4.91 ± 0.08	1.67	98.10
15	14.5 ± 0.25	1.73	96.94
I3C Interday (n = 4)			
0.25	0.26 ± 0.03	12.9	103.44
5.0	4.86 ± 0.28	5.72	97.10
15	14.8 ± 0.25	1.66	98.88
DIM Intraday (n = 6)			
0.25	0.28 ± 0.01	2.35	114.11
5.0	5.40 ± 0.12	2.15	108.02
15	14.5 ± 0.19	1.28	96.83
DIM Interday (n = 4)			
0.25	0.28 ± 0.03	11.66	112.14
5.0	5.27 ± 0.09	1.86	105.38
15	14.8 ± 0.09	0.58	98.98

Data are presented as mean ± SD

Table 3.2

Stability of I3C and DIM in plasma at various experimental conditions

Stability Sample	I3C 0.5 μg/mL	I3C 20 μg/mL	DIM 0.5 μg/mL	DIM 20 μg/mL
			% Remaining	
(a) 24 hours at room temperature				
Mean ± SD	90.83 ± 2.90	88.97 ± 1.51	100.27 ± 1.44	95.13 ± 1.28
RSD (%)	3.19	1.69	1.43	1.34
(b) Autosampler Stability - 24 hours				
Mean ± SD	103.0 ± 4.57	100.00 ± 6.78	98.21 ± 13.35	101.72 ± 5.83
RSD (%)	4.43	6.78	13.59	5.73
(c) Three Freeze-Thaw Cycles				
Mean ± SD	103.3 ± 1.32	91.93 ± 1.12	107.29 ± 5.26	94.78 ± 0.57
RSD (%)	1.28	1.22	4.91	0.60

SD: standard deviation; RSD: relative standard deviation

Table 3.3

Non-compartmental pharmacokinetic parameters of I3C and DIM in Rats

I3C	**CL** **L/h/kg**	**Vd_{ss}** **L/kg**	**$T_{1/2}$** **h**	**AUC_{0-t}** **µg.h/mL**
25 mg/kg IV (n = 4)	33.9 ± 5.6	38.1 ± 26.0	1.62 ± 0.52	0.62 ± 0.14
50 mg/kg IP (n = 6)	2.15 ± 0.4	0.64 ± 0.52	0.64 ± 0.33	23.9 ± 4.43
100 mg/kg IP (n = 4)	120 ± 16	219 ± 30	1.63 ± 0.37	0.71 ± 0.06

DIM	**CL** **L/h/kg**	**Vd_{ss}** **L/kg**	**$T_{1/2}$** **h**	**C_{max}** **µg/ml**	**T_{max}** **h**	**AUC_{0-t}** **µg.h/mL**
20 mg/kg IV (n = 4)	1.88 ± 1.02	2.45 ± 0.7	2.94 ± 2.0	---	---	11.9 ± 5.9
200 mg/kg oral (n = 4)	---	---	12.2 ± 4.3	0.58 ± 0.36	2.75 ± 1.5	5.1 ± 2.7
F (%)	7.0 ± 8.4					

Data are presented as mean ± SD**.** CL: clearance, Vdss: volume of distribution under steady state, $T_{½}$: half life, AUC: Area under the curve, C_{max}: maximum concentration, T_{max}: Time to reach maximum concentration, F: absolute bioavailability

Table 3.4

Non-compartmental pharmacokinetic parameters for I3C major metabolites

I3C	Metabolite	CL L/h/kg	Vd_{ss} L/kg	$T_{1/2}$ h	AUC_{0-t} μg.h/mL	MRT_{0-t} h
25 mg/kg IV	**DIM**	1.34 ± 0.47	0.30 ± 0.22	0.62 ± 0.12	19.7 ± 5.8	0.15 ± 0.04
	HI-IM	1.73 ± 0.73	0.21 ± 0.18	0.27 ± 0.13	14.9 ± 5.2	0.09 ± 0.02
50 mg/kg IP	**DIM**	23.5 ± 10.5	18.6 ± 6.01	0.74 ± 0.20	2.28 ± 1.41	0.67 ± 0.24
100 mg/kg IP	**DIM**	1.36 ± 0.37	1.68 ± 0.26	1.02 ± 0.05	72.3 ± 15.36	1.00 ± 0.08
	HI-IM	1.57 ± 0.45	1.13 ± 0.23	0.80 ± 0.10	61.4 ± 13.95	0.68 ± 0.12

Data are presented as mean ± SD. CL: clearance, Vdss: volume of distribution under steady state, $T_{½}$: half life,

AUC: Area under the curve, MRT: mean residence time.

Table 3.5
Compartmental Pharmacokinetic Parameters of I3C and DIM in rats

I3C	**CL**	**Vd_{ss}**	**$AUC_{0-\infty}$**	**CV**	**AIC**	**TWSSR**
	L/h/kg	**L/kg**	**ug.h/mL**	%		
25 mg/kg IV	32.8 ± 4.5	46.5 ± 39.9	0.76 ± 0.10	23.3	-31	0.0006
50 mg/kg IP	2.4 ± 0.85	0.21 ± 0.14	23.1 ± 10.0	1.23	-8.8	0.092
100 mg/kg IP	108 ± 8.6	152 ± 59	0.92 ± 0.07	12.33	-37	0.004
DIM	**CL**	**Vd_{ss}**	**$AUC_{0-\infty}$**	**CV**	**AIC**	**TWSSR**
	L/h/kg	**L/kg**	**ug.h/mL**	%		
20 mg/kg IV	1.81 ± 1.23	1.39 ± 1.69	14.16 ± 6.93	11	-0.98	0.53
200 mg/kg oral	---	---	9.24 ± 0.05	33.27	-11.5	0.13

Data are presented as mean ± SD. CL: clearance, Vdss: volume of distribution under steady state, $AUC_{0-\infty:}$ Area under the curve from time zero to infinity, C_{max}: maximum concentration, CV (%): cross validation percent, AIC: Akaike information criteria, TWSSR: Total weighted square sum of residuals.

References

[1] M.-H. Pan, C.-T. Ho, Chem. Soc. Rev., 37 (2008) 2558–2574.
[2] A. Jemal, R. Siegel, E. Ward, T. Murray, J. Xu, C. Smigal, M.J. Thun, CA Cancer J. Clin., 56 (2006) 106-130.
[3] J.C. Barrett, Environ. Health Perspect. , 100 (1993) 9-20.
[4] S. Yu, A.-N. Kong, Current Cancer Drug Targets, 7 (2007) 416-424.
[5] R.G. Mehta, G. Murillo, R. Naithani, X. Peng, Pharm. Res., 27 (2010) 950-961.
[6] L. Wattenberg, Proc Nutr Soc., 49 (1990) 173–183.
[7] A. Jernal, R. Siegel, J. Xu, E. Ward, CA Cancer J Clin, 60 (2010) 277-300.
[8] J. Rowland, e. al., MMWR Morb. Mortal. Wkly Rep, 53 (2004) 526–529.
[9] M. Hendryx, E. Fedorko, J. Halverson, J Rural Health, 26 (2010) 383-391.
[10] C. Kiyohara, K. Takayama, Y. Nakanishi, J Nucleic Acids, 2010 (2010) 701760.
[11] R. Prasad, S. Singhal, R. Garg, Biosci Trends, 3 (2009) 41-43.
[12] J. Mathers, G. Strathdee, C. Relton, Adv Genet, 71 (2010) 3-39.
[13] M. Sporn, N. Dunlop, D. Newton, J. Smith, Fed. Proc., 35 (1976) 1332-1338.
[14] Y. Surth, Nat Rev Can, 3 (2003) 768-780.
[15] J.D. Seymour, E.E. Calle, E.W. Flagg, R.J. Coates, E.S. Ford, M.J. Thun, Am. J. Epidemiol., 157 (2003) 980-988.
[16] N.J. Temple, Nutr. Res., 20 (2000) 449–459.
[17] W.C. Willett, Science 254 (1994) 532–537. .
[18] W.C. Willett, Science, 296 (2002) 695–698.
[19] M. Hanausek, Z. Walaszek, T. Slaga, Integrative Cancer Therapies 2(2003) 139-144.
[20] T.O. Khor, W.K. Cheung, A. Prawan, B.S. Reddy, A.N. Kong, Mol. Carcinog, 47 (2008) 321-325.
[21] T. Slaga, J. O'Connell, J. Rotstein, e. al., Symp Fundam Cancer Res, 39 (1987) 31-34.
[22] J. DiGiovanni, 47 (1992) 63-128.
[23] L. Wattenberg, Cancer Res, 52 (1992) 2085s-2091s.
[24] H. Hatcher, R. Planalp, J. Cho, F. Torti, , Cell Mol life Sci 65 (2008) 1631-1652.
[25] N. Juge, F. Mithen, M. Traka, Cellular and Molecular Life Sciences, 64 (2007) 1105-1127.
[26] O. Leoni, R. Iori, S. Palmieri, , Biotechnol Bioeng 68 (2000) 660-664.
[27] J. Fahey, Y. Zhang, T. P, Proc. Natl. Acad. Sci., 94 (1997) 10367-10372.
[28] Y. Kuroiwa, Y. Nishikawa, Y. Kitamura, K. Kanki, Y. Ishii, T. Umerura, M. Hirose, Cancer Lett., 241 (2006) 275-280.
[29] F. Chung, C. Conaway, C. Rao, B. Reddy, Carcionogenesis, 21 (2000) 2287-2291.
[30] A. Singh, D. Xiao, K. Lew, R. Dhir, S. Singh, Carcionogenesis, 25 (2004) 83-90.
[31] C. Yang, T. Smith, J. Hong, Cancer Res, 54 (1994) 1982s-1986s.
[32] Y. Zhang, P. Talalay, Cancer Res, 54 (1994) 1976s-1981s.
[33] S. Barcelo, J. Gardiner, A. Gescher, J. Chipman, Carcionogenesis, 17 (1996) 277-282.
[34] Y.S. Keum, S. Yu, P.P. Chang, X. Yuan, J.H. Kim, C. Xu, J. Han, A. Agarwal, A.N. Kong, Cancer Res, 66 (2006) 8804-8813
[35] C. Chen, A. Kong, Free Radic Biol Med, 36 (2004) 1505-1516.
[36] A. Enomoto, K. Itoh, J. Nagayoshi, T. Haruta, T. Kimura, T. O'Connor, M. Harada, M. Yamamoto, Toxicol Sci, 59 (2001) 169-177.
[37] M. Ramos-Gomez, M. Kwak, P. Dolan, K. Itoh, M. Yamamoto, P. Talalay, T. Kensler, Proc Natl Acad Sci USA, 98 (2001) 3410-3415.
[38] Y. Aoki, H. Sato, N. Nishimura, S. Takahashi, K. Itoh, M. Yamamoto, 173 (2001) 154.
[39] J.S. Lee, Y.S. Surh, Cancer Lett, 224 (2005) 171-184
[40] M. Nachshon-Kedmi, S. Yannai, A. Haj, F.A. Fares, Food Chem. Toxicol., 41 (2003) 745–752.
[41] J.O. Nwankwo, Anticancer Res., 22 (2002) 4129–4135.
[42] Y.H. He, M.D. Friesen, R.J. Ruch, H.A. Schut, Food Chem. Toxicol., 38 (2000) 15–23.
[43] D.T. Verhoeven, H. Verhagen, R.A. Goldbohm, P.A. Vanden-Brandt, G. Van-Poppel, Chem. Biol. Interact., 103 (1997) 79–129.
[44] T.A. Broadbent, H.S. Broadbent, Curr. Med. Chem. , 5 (1998) 469–491.
[45] F. Sarkar, Y. Li, Journal of Nutrition, 134 (2004) 3493S-3498S.
[46] C.M. Cover, S.J. Hsieh, S.H. Tran, G. Hallden, G.S. Kim, L.F. Bjeldanes, G.L. Firestone, J. Biol. Chem., 273 (1998) 3838–3847.

[47] G.S. Salomons, H.J. Brady, M. Verwijs-Janssen, J.D. Van Den Berg, A.A. Hart, B.H. Van Den, H. Behrendt, K. Hahlen, L.A. Smets, Int. J. Cancer 71 (1997) 959–965.
[48] M. Anderton, M. manson, R. Verschoyle, A. Gescher, J. Lamb, P. Farmer, W. Steward, M. Williams, Clin Cancer Res, 15 (2004) 5233-5241.
[49] M. Anderton, M. Manson, R. Verschoyle, A. Gescher, W. Steward, M. Williams, D. Mager, Drug Metab Dispos, 32 (2004) 632-638.
[50] G. Reed, D. Arneson, W. Putnam, H. Smith, J. Gray, D. Sullivan, M. Mayo, J. Crowell, A. Hurwitz, Cancer Epidemiol Biomarkers Prev, 15 (2006) 2477-2481.
[51] G. Reed, J. Sunega, D. Sullivan, J. Gray, M. Mayo, J. Crowell, A. Hurwitz, Cancer Epidemiol Biomarkers Prev, 17 (2008) 2619-2624.
[52] T.C. Chou, Pharmacol. Rev., 58 (2006) 621–681
[53] S. Nair, V. Hebbar, G. Shen, A. Gopalakrishnan, T.O. Khor, S. Yu, C. Xu, A.N. Kong, Pharm Res, 25 (2008) 387-399
[54] G. Shen, T.O. Khor, R. Hu, S. Yu, S. Nair, C.T. Ho, B.S. Reddy, M.T. Huang, H.L. Newmark, A.N. Kong, Cancer Res. , 67 (2007) 9937–9944.
[55] K. Cheung, T.O. Khor, A.N. Kong, Pharmaceutical Research, 26 (2009) 224-231.
[56] S. Roberts, xenobiotica, 31 (2001) 557-589.
[57] T.O. Metz, Q. Zhang, J.S. Page, Y. Shen, S.J. Callister, J.M. Jacobs, R.D. Smith, Biomark Med., 1 (2007) 159-185.
[58] K. Dettmer, P.A. Aronov, B.D. Hammock, Mass Spectrom Rev., 26 (2007) 51-78.
[59] http://www.dkfz.de/en/tox/c010-2_projects/list_assays.html (date of accesss: Nov 5, 2010).
[60] R. Chan, K. Lok, J. Woo, Mol Nutr Food Res, 53 (2008) 201-216
[61] T.K. Lam, L. Gallicchio, K. Lindsley, M. Shiels, E. Hammond, X.G. Tao, L. Chen, K.A. Robinson, L.E. Caulfield, J.G. Herman, E. Guallar, A.J. Alberg, Cancer Epidemiol Biomarkers Prev 18 (2009) 184-195.
[62] L. Tang, G.R. Zirpoli, K. Guru, K.B. Moysich, Y. Zhang, C.B. Ambrosone, S.E. McCann, Cancer Epidemiol Biomarkers Prev 17 (2008) 938-944
[63] A.Y. Arikawa, D.D. Gallaher, J Nutr 138 (2008) 526-532.
[64] C. Chan, H.J. Lin, J. Lin, Int J Oncol 33 (2008) 415-419
[65] P. Talalay, Biofactors, 12 (2000) 5-11
[66] M. Zhu, W.E. Fahl, Biochem Biophys Res Commun, 289 (2001) 212-219.
[67] W.S. Jeong, Y.S. Keum, C. Chen, M.R. Jain, G. Shen, J.H. Kim, W. Li, A.N. Kong, J Biochem and Mol Biol 38 (2005) 167-176
[68] A. Prawan, Y.S. Keum, T.O. Khor, S. Yu, S. Nair, W. Li, L. Hu, A.N. Kong, Pharm Res, 25 (2008) 836-844.
[69] K. Itoh, T. Chiba, S. Takahashi, T. Ishii, K. Igarashi, Y. Katoh, e. al, Biochem Biophys Res Commun, 236 (1997) 313-322.
[70] Y.J. Surh, K.S. Chun, Adv Exp Med Biol, 595 (2007) 149-172.
[71] J. Cao, Y. Liu, L. Jia, H.M. Zhou, Y. Kong, G. Yang, L.P. Jiang, Q.J. Li, L.F. Zhong, Free Rad Biol & Med 43 (2007) 968-975
[72] B.S. Reddy, Subcell Biochem, 42 (2007) 213-225
[73] F.H. Sarkar, Y.W. Li, Acta Pharmacol Sin, 28 (2007) 1305-1315.
[74] R. Yu, S. Mandlekar, W. Lei, W.E. Fahl, T.H. Tan, A.N. Kong, J Biol Chem, 275 (2000) 2322-2327.
[75] S.J. McNally, E.M. Harrison, J.A. Ross, O.J. Garden, S.J. Wigmore, Int J Mol Med 19 (2007) 165-172
[76] L. Zhao, M.G. Wientjes, J.L. Au, Clin Cancer Res 10 (2004) 7994-8004
[77] Y. Zhang, P. Talalay, C.G. Cho, G.H. Posner, Proc Natl Acad Sci USA 89 (1992) 2399-2403
[78] A.N. Kong, R. Yu, V. Hebbar, C. Chen, E. Owuor, R. Hu, R. Ee, S. Mandlekar, Mutat Res, 480 (2001) 231-241
[79] M.K. Kwak, P.A. Egner, P.M. Dolan, M. Ramos-Gomez, J.D. Groopman, K. Itoh, M. Yamamoto, T.W. Kensler, Mutat Res, 480 (2001) 305-315
[80] J.H. Kim, C. Xu, Y.S. Keum, B. Reddy, A. Conney, A.N. Kong, Carcinogenesis, 27 (2006) 475-482
[81] A. Barve, T.O. Khor, X. Hao, Y.S. Keum, C.S. Yang, B. Reddy, A.N. Kong, Pharm Res, 25 (2008) 2181-2189
[82] S. Graham, Cancer Res 43 (1983) 2409s-2413s.
[83] B. Modan, B. Barrell, F. Lubin, M. Modan, R. Greenberg, S. Graham, J Natl Cancer Inst, 55 (1975) 15-18.
[84] J. Cohen, A. Kristal, J. Stanford, J Natl Cancer Inst, 92 (2000) 61-68.
[85] A. Tavani, C.L. Vecchia, Am J Clin Nutr, 61 (1995) 1374S-1377S.
[86] N. Telang, M. Katdare, H. Bradlow, M. Osborne, J. Fishman, Proc Soc Exp Bio Med, 216 (1997) 246-252.
[87] C. Bradfield, L. Bjeldanes, J Toxicol Environ Health, 21 (1987) 311-323.
[88] F. Yuan, D. Chen, K. Liu, D. Sepkovic, H. Bradlow, A. K, Anticancer Res, 19 (1999) 1673-1680.

[89] L. Wattenberg, W. Loub, Cancer Res 38 (1978) 1410-1413.
[90] H. Bradlow, J. Michnovicz, N. Telang, M. Osborne, Carcinogenesis, 12 (1991) 1571-1574.
[91] J. Nixon, J. Hendricks, N. Pawlowski, C. Pereira, R. Sinnhuber, G. Bailey, Carcinogenesis, 5 (1984) 615-619.
[92] R. Dashwood, A. Fong, D. Williams, J. Hendricks, G. Bailey, Cancer Res, 51 (1991) 2362-2365.
[93] B. Pence, F. Buddingh, S. Yang, J Natl Cancer Inst, 77 (1986) 269-276.
[94] K. Grose, L. Bjeldanes, Chem Res Toxicol, 5 (1992) 188-193.
[95] D. Stresser, D. Williams, D. Griffin, G. Bailey, Drug Metab Dispos, 23 (1995) 965-975.
[96] M. Nachshon-Kedmi, S. Yannai, S. Fares, Br J Cancer, 91 (2004) 1358-1363.
[97] I. Chen, A. McDougal, F. Wang, S. Safe, Carcinogenesis, 19 (1998) 1631-1639.
[98] M. Anderton, R. Jukes, J. Lamb, M. Manson, A. Gescher, W. Steward, M. Williams, J Chromatogr B Analyt Technol Biomed Life Sci, 787 (2003) 281-291.

CURRICULUM VITAE

EDUCATION

Rutgers, The State University of New Jersey, NJ

M.S Pharmaceutical Sciences, 2011

Kean University, NJ

B.S Biotechnology, 2004

Minor in Chemistry, 2004

WORK EXPERIENCE

SEPTEMBER 2004-DECEMBER 2010

Rutgers, The State University of New Jersey
Graduate Student, M.S; Department of Pharmaceutics

APRIL 2008-PRESENT

Johnson & Johnson Consumer Inc., PA
Senior Scientist, Research & Development Department

JULY 2007 – APRIL 2008

Rhodia Inc., PA
Research Scientist, Synthesis & Development Department

JANUARY 2007-JULY 2007

Fabricolor Holding Inc, NJ
Senior Scientist, Analytical & Formulation Department

NOVEMBER 2004 - DECEMBER 2006

Epolin, NJ
Chemist, Synthesis, Formulation & Analytical Department

APRIL 2002 - OCTOBER 2006

Princeton Polymer Laboratories, NJ
R&D Associate, Research & Development Department